4-2012

Functional Morphology of the Spiracle and Surrounding Structures of the Spiny Dogfish Shark, Squalus acanthias

Clint McFerren

Functional Morphology of the Spiracle and Surrounding Structures of the Spiny Dogfish Shark, *Squalus acanthias*

by

S. Clint McFerren

Undergraduate Honors Thesis

Directed by

Dr. Dominique G. Homberger
Professor
Department of Biological Sciences

Submitted to the LSU Honor's College in partial fulfillment of the
Upper Division Honor's Program

April 2012

Louisiana State University and Agricultural & Mechanical College
Baton Rouge, Louisiana

Abstract

Benthic, slow-swimming sharks ventilate using a dual pump mechanism, in which water is taken into the oropharyngeal cavity first through the spiracle and then through the mouth. The water is then expressed into the gill chambers and across the gills, where gas exchange takes place, while the mouth, spiracle, and gill slits close and the oropharyngeal cavity is compressed. To begin the ventilatory cycle again, the spiracle opens prior to the mouth (Hughes 1960), but the opening and closing mechanism of the spiracle has remained unknown. Our aim was to elucidate this mechanism through microdissection and imaging of the Spiny Dogfish Shark, *Squalus acanthias*. The spiracle is opened and closed by the spiracular flap, which is formed by the spiracular muscle, which originates from the otic capsule and inserts on the adductor mandibulae process of the palatoquadrate. An elastic spiracular ligament attaches to the spiracular flap at its rostroventral corner and is probably anchored to two radial spiracular cartilages on the internal side of the spiracular flap. When the mouth and spiracle are closed, the spiracular muscle is contracted, wide, and flat, and the elastic spiracular ligament is stretched. In preparation for opening the mouth, the epibranchial musculature contracts and raises the chondrocranium. This stretches, elongates, and narrows the relaxed spiracular muscle and thereby opens the spiracle and breaks the watertight seal within the oropharyngeal cavity. At the same time, the elastic spiracular ligament is released and returns the spiracular muscle to its curved and retracted conformation. As the mouth opens, the palatoquadrate with the adductor mandibulae process and the insertions of the spiracular muscle is protracted, thereby further stretching the spiracular muscle and further increasing the aperture of the spiracle. When the mouth closes, the palatoquadrate with the adductor mandibulae process and the insertion of the spiracular muscle are retracted by the contraction of the levator palatoquadrati, spiracular and rostral levator hyomandibulae muscles. The contracting spiracular muscle, in particular, shortens and bulges, thereby bulging out the spiracular flap and closing the spiracle.

Table of Contents

1. Introduction

In the Spiny Dogfish Shark (*Squalus acanthias*) and most other elasmobranchs with distinct spiracles, gill ventilation is accomplished by a double-pump mechanism (Hughes 1960; Homberger & Walker 2004). The original model proposed by Hughes (1960) has been accepted for almost fifty years, presenting this oropharyngeal pump as the force behind a unidirectional, continuous flow of water over the gills based on pressure differences and suction pumps. Slow-swimming, benthic sharks, such as *Squalus acanthias*, appear to use a pump-based system of gill ventilation because they do not swim fast enough to ram ventilate with an open mouth as some larger pelagic sharks do.

In the dual pump system observed in *Squalus acanthias*, water is taken into the oropharyngeal cavity by first opening the spiracle and subsequently the mouth due to a lower pressure within the oropharyngeal cavity. This sequence by which water enters the oropharyngeal cavity was confirmed by Hughes (1960) as the pressure differences that cause water to enter the oropharyngeal cavity were measured to be initially greater in the spiracle than in the oropharyngeal cavity. As water flows in, the oropharyngeal cavity expands. Next, the mouth and the paired spiracles close, and the oropharyngeal cavity is compressed, which pushes the water into the gill chambers and eventually out of the gill slits until the pressure gradient is at zero or, in some cases, reversed (Hughes 1960; Homberger & Walker 2004). Darbishire (1907) was able to show that the water entering the spiracle of the Spiny Dogfish Shark exits through the first two or three gill slits, whereas the water entering the mouth exits through the posterior three gill slits. This observation in itself supports the idea that the spiracle opens prior to the mouth. Once the water is pushed out of the gill slits, the spiracle, mouth, and gill slits close, which, together with the compression of the oropharyngeal cavity, leaves a watertight space at negative pressure within the oropharyngeal cavity and the gill and parabranchial chambers (Hughes, 1960). The Spiny Dogfish Shark, in this condition, is unable to open its mouth, unless the spiracle opens first to allow at least a tiny amount of water to enter the oropharyngeal cavity in order to eliminate the negative pressure and break the seal, so that the mouth can be opened, and the ventilation process can be repeated (Hughes 1960; D.G. Homberger personal communication).

However, recent findings suggest that water flow across the gills is not always unidirectional in elasmobranchs (Ferry-Graham 1999), leading to the proposal of a modified model by Summers and Ferry-Graham (2001). At some time during the pumping cycle, the pressure in the oropharyngeal cavity is lower than the pressure in the parabranchial cavity after the water has been pushed through the gill chambers (Hughes 1960; Ferry-Graham 1999). Although Hughes (1960) was aware of this, a lack of technology at that time kept him from being definite in how to interpret such a pressure reversal. Lauder (1983) suggested that the gill arches located between the oropharyngeal cavity and parabranchial cavity are capable of impeding flow reversal by moving closer together. However, Ferry-Graham and Summers (2003) were able to confirm an actual flow reversal of water from the parabranchial cavity into the oropharyngeal cavity through the use of endoscopic video data. Their findings suggest that the gill arches do not always compress tightly enough to eliminate water flow from the parabranchial chamber to the oropharyngeal cavity. More specifically, they were able to show that the openings between the oropharyngeal cavity and gill chambers closed sufficiently to prevent water flow only about halfway through the pressure reversal, which confirms that a flow reversal does happen for at least the first half of the total pressure reversal. Summers and Ferry-Graham (2003) also found that water does not enter the parabranchial cavity through the external gill slits. The model presented by Summers and Ferry-Graham (2003) shows that the flow of water across the gills is not continuous, at times stopping, or even returning to the oropharyngeal cavity from the parabranchial chambers.

The question then arises as to how sharks prevent water flow into the gills from the external medium. Bony fishes use the operculum, a large, single bone covered by skin, to close off the gill chambers externally and prevent water from reentering through the external gill slits. The operculum originates from the hyoid arch and covers the gills (Liem et al. 2001). However, an operculum is not present in cartilaginous fishes, such as the Spiny Dogfish Shark, which use the trematic constrictor muscles to close the external flap valves of the five gill slits in the Spiny Dogfish Shark (Homberger & Walker 2004).

With respect to the effect of a momentary flow reversal on the efficiency of oxygen extraction, Piiper and Schumann (1967) were able to show that there was none, because most of

the time, oxygen (PO_2) levels in the branchial arteries were much higher than in the water leaving the gills.

Many sharks tend to utilize ram ventilation during which water is forced into the open mouth and then through the open gills while swimming. This type of ventilation is utilized by large fast-swimming pelagic shark species, in which the spiracle is either reduced or lost and in which water enters the oropharyngeal cavity because of the speed at which they swim, as well as other larger species with spiracles, such as whale sharks and basking sharks, in which water enters the oropharyngeal cavity easily because of their large mouths (Homberger & Walker 2004).

Theoretically, ram ventilation would seem more efficient as water is continuously driven across the gills at a constant rate and a countercurrent optimum exchange of oxygen is maintained. However, Malte (1992) showed that the anatomy of the gills in most sharks is configured in a manner in which there is only a 3% drop in efficiency of oxygen extraction in a pulsatile flow of water across the gill tissue as compared to a continuous flow. Therefore, what is lost in the continuity of water flow is made up for in the increased ability of the gills to remove oxygen from the water.

The kinetic skull and attaching muscles of sharks work together as a functional unit in both feeding and ventilation. The spiracle is located between the first (mandibular) and second (hyoid) branchial arches of the Spiny Dogfish Shark (Hamlett 1999). Externally, it is positioned laterodorsally between the rostrally located levator palatoquadrati and spiracular muscles and the caudally located levator hyomandibulae muscle. Internally, the opening of the spiracle in the oropharyngeal cavity is located on the rostral end of the roof of the oropharyngeal cavity in front of the internal opening of the five gill slits (Homberger & Walker 2004). The opening and closing of the spiracle are most likely not primary movements, but rather the by-product of other movements within the skull. If this argument is correct, these movements must be achieved by an active mechanism, a conclusion first proposed by Hughes (1960). However, the precise mechanism of the opening and closing of the spiracle has yet to be elucidated.

The aim of my project is to discover the anatomical structures that are responsible for the active opening and closing of the spiracle. The function of the spiracle has not and cannot be fully grasped until its anatomy is properly analyzed, described, and functionally interpreted.

2. Materials & Methods

2.1. Materials

Eight preserved specimens (six females and two males) of the Spiny Dogfish Shark (*Squalus acanthias*) were obtained from NASCO Biological Supply Company in Fort Atkinson, Wisconsin (Table 1). Most of the larger sharks were females, which tend to be larger than males. The only male juvenile specimen was easily identifiable because of his incompletely developed claspers, which are a sign of sexual immaturity (Stenberg 2005).

The degree of openness of the spiracle was classified into five stages: Open, almost open, half closed, almost closed, and closed (Table 1). An "open" spiracle indicates that the spiracular flap is retracted, allowing the entire spiracular opening to be exposed and capable of water intake. An "almost open" spiracle indicates that the spiracular flap is partly covering the opening of the spiracle, while about three-fourths of the opening is still clear and available for water intake. A "half closed" spiracle indicates that the spiracular flap is covering approximately half of the spiracular opening. An "almost closed" spiracle indicates that the spiracular flap has nearly covered the opening, which is still capable of some water intake. And lastly, a "closed" spiracle indicates that the flap has completely closed the spiracular opening, thereby creating a watertight space within the oropharyngeal cavity and branchial pouches, when the mouth and gill slits are closed. Shark specimens with spiracles in a variety of positions were selected in order to gain a holistic perspective on the possible movements of the spiracular flap (Table 1).

All specimens were stored in a 1% 4-phenoxyethanol solution. After they were removed from the holding tank for dissection, they were kept moist by spraying them with the same solution from squirt bottles.

2.2. Methods

Two pairs of watchmaker's forceps were used to perform the dissection of the spiracle. One pair was obtained from Carolina Biological Supply Company (Burlington, North Carolina) and the other from VWR International (Radnor, Pennsylvania). The stainless steel forceps were manually sharpened under a stereomicroscope, using a natural black Arkansas novaculite stone (Dan's Whetstone Company, Pearcy, Arkansas) to ensure that the forceps had sharp tips and smooth edges necessary for a neat, precise microdissection under a stereomicroscope.

Two stereomicroscopes (Wild M4 TYP 45510, Leica, Heerbrugg, Switzerland) were used for sharpening the forceps and for performing the microdissection. One stereomicroscope was fitted with a dual ocular discussion tube. In order to illuminate the specimen, the stereomicroscopes were also fitted with a fiber optic ring light (Volpi, Schlieren, Switzerland) with a light-polarizing filter and connected to a lightbox (Intralux 6000 or HCL 150, Volpi USA, Auburn, NY). The dissection was performed under high magnification (6.5× or 16×).

Initial observations were made by noting the details of the surface morphology of the open spiracle, and supporting digital images were taken. Next, the dissection was completed in a stepwise manner, with digital images being taken at each step. First, the skin was removed from the area surrounding the spiracle, leaving the superficial fascia on the shark. Second, the superficial fascia was removed to expose the underlying muscles. Once the muscles were cleaned of loose connective tissue and epimysia, it was possible to note the exact origins, insertions, and fiber directions of the muscles surrounding the open spiracle, so that the action of the muscles could be inferred.

Mesoscopic photographs of the shark specimens were taken using an A SPOT Insight Firewire Camera and Leica MZ8 microscope. Image processing was done through the ImagePro version 5.5 software (Media Cybernetics, Bethesda, MD). This software was used to create extended depth of field (EDF) images with a fully focused image of three-dimensional objects through a series of images at different focal positions, which were merged into a composite image that is entirely focused. Vibrations were eliminated by placing the stereomicroscope and specimen on a micro-g anti-vibration table (Technical Manufacturing Corporation, Reabody, MA). Compressed nitrogen from a nitrogen tank was used to float the table and, thus, dampen

any vibrations, which would have blurred the image. The software Adobe Photoshop CS4 was used to further process the images by correcting the color levels. Once a satisfactory digital image had been taken, a second digital image was taken with a metric scale placed in the area of focus. This had two purposes. The first was to ensure that the photograph was actually focused and the magnification was recorded. The second was to create a scale bar of specific length for the image to be included in a publication. Using the image with the focused scale, a scale bar was made by measuring the number of pixels between the marks on the scale. For example, the number of pixels between two grid marks equaling one millimeter will be the same in both images. The designed scale bar was then transferred to the first image to show the realistic size of the imaged object irrespective of the magnification used in the publication.

Macroscopic digital images of the shark specimens were taken with a SPOT Insight Color Closed-Circuit TV Camera and SPOT Advanced Imaging Software (Diagnostic Instruments, Sterling Heights, Michigan). Two separate lenses were used to provide different fields of view and levels of magnification. A 45 mm lens was used for the close-up pictures, and a 14.5 mm lens was used for the pictures of the entire length of the shark's body. The camera was mounted on a Bencher copy stand (Bencher, Inc., Antioch, Illinois), which allowed for a stable base and easy vertical adjustment of the overhead camera. The copy stand was equipped with an Illuma System Light Control 8 and four Sun-Lite UL E196560 Portable Luminaires, each with an attached GE Reveal 140 watt/140 volt incandescent bulb coated in neodymium. The lights were oriented in different angles to illuminate particular structures and to provide even lighting. When needed, diffusers, or sheets of translucent Plexiglas, were placed in front of the light bulbs to even out or reduce the amount of light. When taking the digital images, the neon ceiling lights were turned off to reduce flickering and glare.

All digital images were labeled by using the software Adobe Photoshop CS4.

3. Results: Morphological Description

3.1. Surface and Skin

The skin surrounding the spiracle is of even thickness, yet variable in its adherence to the underlying superficial fascia. On the rostral side of the spiracle, the skin closely adheres to, and is very difficult to separate from, the superficial fascia. On the dorsal side of the spiracle, the

skin maintains a relatively tight adherence to the superficial fascia, but not to the same degree as on the rostral side. On the ventral side of the spiracle, the skin is as thick as that on the rostral and dorsal sides, but adheres less tightly and variably to the superficial fascia. On the caudal side of the spiracle, the skin seems to be slightly thinner and is only loosely connected to the underlying superficial fascia.

Numerous surface pores leading to the mandibular pit organs, which are part of the lateral line system (Homberger & Walker 2004), are arranged in two rows that run from cranioventral to caudodorsal caudal to the spiracle (Figs. 1B, 5 and 6A). Some light-gray marks on the skin surrounding the spiracle of some specimens may be scars from injuries (Fig. 2B).

Near the spiracle, the skin maintains its texture and appearance up to the edges of the spiracular opening before it turns into a thin epithelium, which lines the walls of the spiracular canal (Fig. 3). Thus, a divide is created between the tough external skin with placoid scales and the thin, pliable internal epithelium lacking scales (Fig. 3).

The dorsal and rostral edges of the spiracular opening are sharp-edged and stiff (Fig. 5). They are supported by a halfmoon-shaped cartilage that is anchored in the superficial fascia of the caudodorsal corner of the spiracular opening and extends ventrally along the rostral spiracular edge to attach to the superficial fascia enveloping the adductor mandibulae muscle (Fig. 6A, B). On the rostral side of the spiracle, the skin continues over the edge, doubling back and forming a pouch before enveloping the spiracular flap and then continuing to cover the rest of the spiracular canal down to the oropharyngeal cavity (Figs. 6 and 8). The skin of the ventral edge of the spiracular opening is softer and tangentially folded (Figs. 2B, 3 and 4). The caudal edge of the spiracular opening is blunt and slightly S-shaped in its outline with an indentation into which the spiracular flap did fit in a closed spiracle (Fig. 4). The epithelium that covers this indentation is thin, scaleless, and tightly adhered to the underlying tissue (Fig. 4).

3.2. Superficial Fascia

Directly underneath the skin lies the superficial fascia, a strong and fibrous collagenous connective tissue, whose fiber direction varies. Dorsal to the spiracle, the collagen fiber bundles run from craniodorsal to caudoventral (Fig. 5); the muscle fiber bundles of the underlying levator palatoquadrati and spiracular muscles run crosswise to the fiber bundles of the overlying

superficial fascia, namely from cranioventral to caudodorsal (Figs. 6 and 7). On the caudal side of the spiracle, the collagen fiber bundles of the superficial fascia run from cranioventral to caudodorsal (Fig. 5), which is slightly crosswise with the fibers of the underlying caudal levator hyomandibula muscle, which run from dorsal to ventral (Figs. 6, 7 and 8). The point of change in the fiber direction of the superficial fascia from the dorsal edge to the caudal edge of the spiracular opening occurs at approximately the same point at which the underlying spiracular muscle meets the levator hyomandibulae muscle (Figs. 5 and 6). On the rostral side of the spiracle, the fiber direction of the thick and tough superficial fascia is indistinct (Fig. 5). On the ventral side of the spiracle, the connective tissue of the superficial fascia is relatively thin, with the bulky adductor mandibulae muscle bulging under and being visible in certain places where the superficial fascia is thin and translucent (Fig. 5). On the ventral and caudal sides of the spiracle, the edges are blunted and gradually curve into the spiracular canal (Figs. 5 and 6A). The fat tissue along the ventral edge of the spiracular opening is loosely connected to the surface of the superficial fascia (Fig. 5), whereas the fat tissue along the caudal edge of the spiracular opening is substantial and tightly connected to the underside of the superficial fascia (Fig. 6C).

3.3. Muscles

The branchiomeric muscles and associated structures surrounding and affecting the spiracle are complex. The spiracle is bordered on its rostral side by the spiracular and levator palatoquadrati muscles and on its caudal side by the large levator hyomandibulae muscle (Figs. 7 and 8). Ventral to the spiracle is the bulging adductor mandibulae muscle, which adducts the upper and lower jaw (Fig. 8A).

The adductor mandibulae muscle overlies the palatoquadrate cartilage, the more ventrally located mandibular cartilage, and parts of the more caudodorsally situated hyomandibula and complex jaw joint at which the three skeletal elements articulate (Fig. 8B). The hyomandibular nerve trunk of the facial nerve (VII) emerges from the side of the chondrocranium slightly ventral to the inner ear and runs underneath the epithelium lining the wall of the spiracular canal (Figs. 9, 10 and 11). As it travels out of the caudal edge of the spiracular canal, it crosses the lateral side of the levator hyomandibulae muscle and the laterally exposed portion of the hyomandibula, where it branches and sends nerve fiber bundles rostroventrally across the adductor mandibulae muscle and caudoventrally towards the hyoid constrictor muscles (Figs. 6,

7 and 8A). Beneath the nerve lies the levator hyomandibulae muscle, which seems to be held in a slightly curved position by the strong hyomandibular nerve trunk (Figs. 7 and 10). The hyomandibular nerve trunk seems to hold the levator hyomandibulae muscle in a slightly curved back position and actually makes an indentation in the lateral surface of the cranial levator hyomandibulae muscle (Fig. 10).

The preorbital muscle originates from the underside of the rostrum and inserts by three tendons in association with the ventral portion of the adductor mandibulae muscle and the mandibular branch of the trigeminal nerve (V), which runs along the rostral border of the adductor mandibulae muscle, passes over the dorsal labial cartilage, and continues into the oropharyngeal cavity (Figs. 12 and 13). The lateral tendon bundle is superficial to the mandibular branch of the trigeminal nerve (V) and inserts onto the rostrolateral side of the adductor mandibulae muscle (Fig. 12). The middle tendon bundle is the strongest one. It lies deep to the mandibular branch of the trigeminal nerve (V) and inserts onto the medial surface of the adductor mandibulae muscle (Fig. 12 and 13). The deepest and smallest tendon attaches to the lateral surface of the mandibular cartilage underneath the adductor mandibulae muscle (Fig. 13).

The complex levator hyomandibulae muscle, which lies along the caudal edge of the spiracle, comprises two main components, namely the rostral and caudal levator hyomandibulae muscles (Figs. 8, 14 and 15). The large caudal levator hyomandibulae muscle is simple; it originates from the superficial fascia covering the epibranchial musculature and inserts on the laterodorsal surface of the hyomandibula (Fig. 16). The rostral levator hyomandibulae muscle is divided into a superficial and a deep portion. The superficial portion forms the caudal border of the spiracle and originates from the laterodorsal edge of the otic capsule (Fig. 15). It inserts mostly onto the medial side of the adductor mandibulae process of the palatoquadrate, but some of its muscle fibers insert on the underlying aponeurosis of the palatoquadrate part of the deep portion of the rostral levator hyomandibulae muscle (Fig. 15). The deep portion in turn comprises two parts with distinct attachments, namely the palatoquadrate part and the hyomandibular part (Fig. 16). The palatoquadrate part is superficial to the hyomandibular part and originates from the side of the otic capsule of the chondrocranium. This part runs along the hyomandibula, becomes tendinous at midlength, and then becomes muscular again before

inserting onto the medial side of the adductor mandibulae process of the palatoquadrate as well as onto the aponeurosis that separates the rostral levator hyomandibulae muscle from the spiracular opening (Fig. 16A). Deep to the palatoquadrate part is the hyomandibular part of the deep portion of the rostral levator hyomandibulae muscle, which originates on the side of the otic capsule of the chondrocranium ventral to the origin of the palatoquadrate part and inserts onto a process located on the dorsal surface of the hyomandibula.

The afferent spiracular artery, which originates from the pretrematic branch of the first collector loop (Homberger & Walker 2004), runs longitudinally over the lateral surface of the hyomandibula at the level of the complex jaw joint before slipping underneath the palatoquadrate part of the deep portion of the rostral levator hyomandibulae muscle. As it enters the spiracular canal, it supplies the pseudobranch on the internal surface of the rim of the rostral and rostroventral sections of the spiracular flap formed by the spiracular muscle (Figs. 17 and 18). The efferent spiracular artery leaves the pseudobranch and continues along the wall of the spiracle (Fig. 18), eventually joining the carotid artery in the cranial cavity (Homberger & Walker 2004).

In the open position of the spiracle, the spiracular muscle is retracted and stands up in its rostral and rostroventral sections (Figs. 7 and 10). At the rostroventral bend underneath the spiracular pouch, the elastic rostral spiracular ligament attaches to the spiracular muscle (Figs. 7 and 8) and is probably anchored to the two radially arranged spiracular cartilages, which support the internal side of the spiracular flap (Figs. 18 and 19). The shorter ventral spiracular ligament connects the ventral side of the spiracular muscle to the mediodorsal side of the adductor mandibulae process of the palatoquadrate cartilage (Fig. 14). This ligament is stronger and contains more collagenous connective tissue fibers than the rostral spiracular ligament. These two ligaments maintain the curved shape of the spiracular muscle in its open configuration (Figs. 9 and 14).

Underneath the marginal cartilage and superficial fascia, the spiracular muscle, which forms the spiracular flap, is covered by a thin epithelium with few small scales (Figs. 6 and 8A). In the open position of the spiracle, the spiracular muscle is retracted and stands up in its rostral and rostroventral sections (Figs. 7 and 10). At the rostroventral bend underneath the spiracular pouch, the elastic rostral spiracular ligament attaches to the spiracular muscle (Figs. 7 and 8) and

is probably anchored to the two radially arranged spiracular cartilages, which support the internal side of the spiracular flap (Figs. 18 and 19). The shorter ventral spiracular ligament connects the ventral side of the spiracular muscle to the mediodorsal side of the adductor mandibulae process of the palatoquadrate cartilage (Fig. 14). This ligament is stronger and contains more collagenous connective tissue fibers than the rostral spiracular ligament. These two ligaments maintain the curved shape of the spiracular muscle in its open configuration (Figs. 9 and 14).

The spiracular muscle is curved when the spiracle is open. It originates on the otic capsule, caudally extending underneath the origin of the levator hyomandibulae muscle, and inserts on the medial surface of the adductor mandibulae process of the palatoquadrate deep to the insertion of the superficial portion of the levator hyomandibulae muscle (Figs. 17 and 18). At the origin and insertion of the spiracular muscle, the muscle fibers diverge widely and cover a wide area, in contrast with the narrow and upright middle section of the muscle when the spiracle is open. Two cartilages lie underneath the pseudobranch and its arteries on the internal surface of the spiracular muscle and are oriented perpendicularly to the muscle fiber direction of the spiracular muscle (Fig. 19). The ventral spiracular cartilage is approximately twice as wide as the other cartilage. The cartilages are embedded in a tough connective tissue that keeps them adhered to the inner wall of the spiracular muscle. They presumably reinforce and support the spiracular muscle on its internal side and probably serve as insertion places for the two spiracular ligaments.

4. Discussion

The complex arrangement of the muscles and structures surrounding the spiracle are configured in such a way as to contribute to the functioning of the spiracle.

It is interesting to note that degree of openness of the spiracles in two of the specimens (SCM007, SCM008) was asymmetrical. This could be a natural occurrence or the result of preservation and storage; either way, it is worthy of thought and further investigation.

The skin surrounding and lining the spiracle is a great example of how form fits function. The scaly skin external to the spiracle is tough and protects the edges and the area surrounding the spiracle from mechanical trauma. This can be inferred from the scars that were observed in some specimens in our study. The skin that covers the external side of the spiracular flap is

thinner than the external skin and bears fewer, smaller scales. It is likely that this scaly, though thin skin evolved because it may be subject to mechanical abrasions when the spiracular flap is closed, but is protected when the spiracular flap is retracted underneath the rostral edge of the spiracle. The thin and less scaly skin conforms more closely to surrounding structures when the spiracular flap is retracted into the spiracular pouch. The skin of the spiracular pouch is somewhat elastic and wrinkled when the spiracle is open. As the spiracular flap moves caudally to close the spiracle, the skin of the spiracular pouch will straighten and tighten. The epithelium lining the spiracular canal is thin and smooth, being well suited for enhancing the flow of water. The spiracular groove on the caudal edge of the spiracle is shaped to accommodate the free edge of the spiracular flap when the spiracle is closed. Its shape and scaleless skin are appropriate for a watertight closure of the spiracular flap, as it forms an indentation that matches the curve of the spiracular flap.

The pseudobranch lines the internal edge of the spiracular flap formed by the spiracular muscle. Traditionally, it has been thought that the pseudobranch is a reduced, yet functioning gill (Homberger & Walker 2004). It is possible that at one point in evolutionary history, the pseudobranch was a fully functional gill, because of its structure and its location in a chamber between the first (mandibular) and second (hyoid) arches. However, upon closer examination, it seems possible that the pseudobranch might rather have a role in the closing of the spiracle (D.G. Homberger personal communication). The pseudobranch protrudes from the internal wall of the spiracular flap and has the appearance of a structure that could conform to the spiracular groove to create a watertight seal when the spiracular flap closes the spiracle. The disproportionately large afferent and efferent spiracular arteries relative to the small pseudobranch raise the possibility that the pseudobranch is an inflatable tissue.

The particular placement of fat tissue around the spiracle also supports the functioning of the spiracle. The fat is located between the skin and superficial fascia along the ventral edge of the spiracle, where the skin is folded tangentially. This skin may be stretched when the spiracular flap is protracted and closes the spiracle. The fat along the caudal edge of the spiracle surrounds the hyomandibular nerve trunk, which lies underneath the superficial fascia. This provides a hydraulic cushion to the nerve and also causes the caudal edge to be soft and slightly adjustable in its shape. This would enhance the ability of the spiracle to close tightly.

The marginal cartilage that brings rigidity to the dorsal and rostral edges of the spiracle offsets the softer caudal and ventral edges. Being located on the side from which the spiracular flap moves to cover the spiracle, this rigidity brings stability to the spiracular structure as a whole. When the spiracular flap moves caudally to close the spiracle, the marginal cartilage ensures that the shapes of the rostral and dorsal edges are maintained. The stability of the marginal cartilage is further supported by its insertion near the tendon of the complexly pinnate adductor mandibulae muscle, which is large and has a low range of motion as well.

The position of the spiracular flap, or the extent to which it covers the spiracular opening, is highly variable in the spiracles of the eight specimens that were examined. This variability demonstrates the mobile nature of the spiracular flap formed by the spiracular muscle. When the spiracle is open, the spiracular muscle is curved, and its caudal edge is curved outwards. The two spiracular ligaments attaching to the spiracular muscle and cartilages play a key role in maintaining the muscle's configuration in the open spiracle. The rostral spiracular ligament is elastic and pliable, and its role is that of an antagonist to the spiracular muscle. As the spiracular muscle straightens, contracts, and thereby moves caudally across the spiracular opening, it has to overcome the resistance of the rostral spiracular ligament, but when this happens, the rostral spiracular ligament will stretch with the muscle because of its elastic nature. Once the muscle relaxes, it no longer overcomes the resistance of the ligament, and the ligament recoils, aiding in the process of bringing the spiracular muscle back into its curved configuration. The ventral spiracular ligament is stiffer and fibrous, suggesting a different role. Its connection to the spiracular muscle is shorter and tighter than that of the rostral spiracular ligament and serves to anchor the spiracular muscle on the medial side of the adductor mandibulae process. It causes the ventral side of the spiracle muscle to closely conform to the medial side of the palatoquadrate cartilage to ensure the curved shape of the spiracular muscle when the spiracle is open. Keeping the spiracular muscle close to the palatoquadrate cartilage, the placement of the ventral ligament also supports the wide but thin insertion of the spiracular muscle onto the medial side of the palatoquadrate cartilage. It can be concluded that the main role of these two ligaments is the preservation of the unique curved shape of the spiracular muscle when the spiracle is open.

The preorbital muscle, originating on the underside of the nasal capsule (Homberger & Walker 2004), protracts the jaw of the Spiny Dogfish Shark by causing an anteriorly directed

force on the jaws. The site of its attachment has been described previously. Wilga and Motta (1998) describe it as inserting to the ventral portion of the adductor mandibulae muscle, whereas Homberger and Walker (2004) suggest that it inserts onto the caudal end of the palatoquadrate. Our study suggests that neither of these descriptions is accurate, as there are actually three points of insertion for the preorbital muscle. Its tripartite insertion is crucial and necessary to its ability to protract the jaw, as it inserts onto the medial and lateral sides of the ventral portion of the adductor mandibulae muscle as well as onto the surface of the mandibular cartilage, so that it pulls the jaw forward when it contracts. The palatoquadrate, mandibular cartilage, hyomandibula, and ceratohyal cartilage are a functional unit. Therefore, when the preorbital muscle pulls on the adductor mandibulae muscle and mandibular cartilage through its tripartite insertion, the palatoquadrate, hyomandibula, and ceratohyal cartilage are pulled along, thus protracting the jaw.

The Spiny Dogfish Shark is able to protrude its jaw almost 30 percent of its head length (Wilga & Motta 1998), which is more than most species of sharks. The anteroposterior alignment of the preorbital muscle is not found in all sharks and is thought to play a large role in this effective protraction. Protraction could be advantageous because it reduces the distance that the lower jaw has to move to close the gape by 51 % (Wilga & Motta 1998). The evolutionary importance of this muscle is clear as the protraction of the jaws causes the gape of the mouth in the Spiny Dogfish Shark to be more efficient for water entry in ventilation and prey capture in feeding.

The levator hyomandibulae muscle works to retract the jaw (Wilga & Motta 1998, Homberger & Walker 2004). Wilga and Motta (1998) and Homberger and Walker (2004) state that the levator hyomandibulae originates from the surface of the epibranchial musculature and the side of the otic capsule. We have found that it actually originates from the superficial fascia of the epibranchial musculature. Wilga and Motta (1998) suggest that the levator hyomandibulae muscle inserts onto the hyomandibula, whereas Homberger & Walker (2004) add that while it inserts on the hyomandibula, it also sends fibers to insert on the palatoquadrate. Once again, we found that its multiple insertions are not so simple and are fundamental in its ability to retract the jaw. The configuration of the levator hyomandibula muscle suggests that the attachment of the levator hyomandibulae muscle to the palatoquadrate, namely the palatoquadrate part of the

superficial portion of the rostral levator hyomandibulae muscle, may have evolved secondarily in order to retract the palatoquadrate, because the spiracular and levator palatoquadrati muscles only raise the palatoquadrate. By attaching the levator hyomandibulae muscle to both the palatoquadrate and the hyomandibula, these two cartilages are linked and work as a functional unit in ventilation and feeding.

Another aspect that is advantageous to the spiracle is the tight placement of the hyomandibular nerve trunk on the rostral edge of the rostral levator hyomandibular muscle. When this nerve trunk was removed, it left a noticeable indentation in the rostral edge and lateral surface of the rostral levator hyomandibulae muscle, leaving one with the impression that the nerve trunk was tying the muscle back from the spiracular opening.

Possibly the most interesting discovery made was the two spiracular cartilages found on the internal side of the spiracular flap formed by the spiracular muscle. They obviously provide support and stability to the shape of the spiracular muscle. It is probable that the rostral spiracular ligament passes between the muscle fiber bundles of the spiracular muscle to insert onto the two spiracular cartilages. It is rare for a ligament to just insert onto the surface of a muscle, and this insertion would provide a stable attachment. This unit, composed of the rostral ligament and the two internal cartilages of the spiracular muscle, is probably foundational to the action of the spiracular muscle and the functioning of the spiracle.

Wilga and Motta (1998) have presented a model for the opening and closing of the jaw, which is based upon three phases; the expansive phase, compressive phase, and recovery phase. During the expansive phase, the epibranchial musculature, which inserts onto the posterodorsal surface of the chondrocranium (Wilga & Motta 1998, Homberger & Walker 2004), contracts to raise the chondrocranium. Additionally, it has been suggested that the coracomandibular muscle pulls down the lower jaw at this time (Wilga & Motta 1998), although this was shown not to be the case upon further study (D.G. Homberger unpublished observations). The labial cartilages will then extend as the oropharyngeal cavity is expanded, and the expansive phase will end at the peak gape (Wilga & Motta 1998). Next, the compressive phase is initiated when the jaw protracts by the contraction of the preorbital muscle, causing the orbital process of the palatoquadrate to move forward along the ethmopalatine groove (Wilga & Motta 1998). The adductor mandibulae then contracts to adduct the upper and lower jaw, closing the mouth (Wilga

& Motta 1998, Homberger & Walker 2004). The recovery phase begins when the mouth is completely closed. The jaw is then retracted by the levator palatoquadrati, spiracular and levator hyomandibulae muscles. Once all of the jaw components and cranial elements are back in their original position, the recovery phase ends (Wilga & Motta 1998).

With the present data, we can hypothesize a mechanism of the opening and closing of the spiracle. The spiracular muscle formed by the spiracular flap is primarily responsible for the opening and closing of the spiracle. Because we know that the opening and closing of the spiracle is connected to the movements of skeletal elements and muscles within the head of the Spiny Dogfish Shark, it is necessary to place the movements of the spiracular muscle into the series of movements of the surrounding cartilages and muscles during the feeding and breathing processes of the Spiny Dogfish Shark.

With respect to the spiracle, its opening and closing are closely correlated with the movements of the spiracular muscle, which originates on the side of the otic capsule and inserts on the medial side of the adductor mandibulae process of the palatoquadrate. When the mouth and spiracle are closed, the spiracular flap is drawn across the spiracular opening as the spiracular muscle is contracted, flat, and wide, thus overcoming the resistance of the elastic rostral spiracular ligament and stretching it. When the epibranchial musculature contracts, the chondrocranium is raised, and the spiracular muscle is stretched, elongated, and narrowed, thereby starting to open the spiracle and breaking the watertight seal within the oropharyngeal cavity. The rostral elastic spiracular ligament is then released, and the spiracular muscle reassumes its curved conformation. As the mouth opens and reaches peak gape, the palatoquadrate with the adductor mandibulae process and insertions of the spiracular muscle is protracted by the contraction of the preorbital muscle, thereby stretching the spiracular muscle and increasing the aperture of the spiracle. While the palatoquadrate is still protracted, the mouth closes by the contraction of the adductor mandibulae muscle. Next, the palatoquadrate with the adductor mandibulae process and the insertions of the spiracular muscle is retracted by the contraction of the levator palatoquadrati, spiracular and rostral levator hyomandibulae muscles. The spiracle once again assumes a tightly closed configuration as the spiracular muscle is contracted, flat, and bulged, fitting in the spiracular groove. The internal oropharyngeal cavity is at negative pressure, and the seal is secured.

This model will have to be tested by studying the anatomy of the closed spiracle as this project was only based upon the dissection of a specimen with an open spiracle.

5. Acknowledgements

I would like to thank Dr. Dominique G. Homberger for advising and funding this project, as she was unwavering in her support and encouragement. Jonathan A. Bonin, Brooke H. Dubansky, and Michelle L. Osborn assisted in taking the photographs and were constantly available to give advice and help. Sigrid N. Hamilton acquired and scanned numerous literature sources that were used for this study. I also thank Dr. Richard E. Condrey and Dr. Fernando Galvez for serving on my Honors committee and for their feedback and suggestions on a draft of the Honors thesis.

6. Literature Cited

Darbishire, A.D. 1907. On the direction of the aqueous current in the spiracle of the dogfish; together with some observations on the respiratory mechanism in other elasmobranch fishes. Journal of the Linnean Society of London, Zoology, 30: 86–94.

Ferry-Graham, L.A. 1999. Mechanics of ventilation in swellsharks,*Cephaloscyllium ventriosum* (Scyliorhinidae). Journal of Experimental Biology 202 (11): 1501-1510.

Hamlett, W.C. 1999. Sharks, skates, and rays: The biology of elasmobranch fish. Johns Hopkins University Press, Baltimore, Maryland. Pp. 174-195.

Homberger, D.G. & Walker, W.F. 2004. Vertebrate Dissection, 9th ed. Brooks/Cole Thompson Learning, Inc., Belmont, California. Pp. 44-47, 133-136, 218-219, 263-265, 302.

Hughes, G.M. 1960. The mechanism of gill ventilation in the dogfish and skate. Journal of Experimental Biology 37: 11-27.

Lauder, G.V. 1983. Functional design and evolution of the pharyngeal jaw apparatus in euteleostean fishes. Zoological Journal of the Linnean Society 77: 1-38.

Liem, K.F., Bernis, W.E., Walker, W.F. & Grande, L. 2001. Functional anatomy of the vertebrates. Harcourt College Publishers, Orlando, Florida. P. 581.

Malte, H. 1992. Effect of pulsatile flow on gas exchange in the fish gill: theory and experimental data. Respiration Physiology 88: 51-62.

Piiper, J. & Schumann, D. 1967. Efficiency of oxygen exchange in the gills of the dogfish, *Scyliorhinus stellaris*. Respiration Physiology 2: 135-148.

Stenberg, C. 2005. Life history of the piked dogfish (*Squalus acanthias*) in Swedish waters. Journal of Northwest Atlantic Fishery Science 35: 155-164.

Summers, A.P. & Ferry-Graham, L.A. 2003. Respiration in elasmobranchs: new models of aquatic ventilation. Pp. 87-100 *in* Vertebrate Biomechanics and Evolution (Bels, V.L., Gasc, J-P. & Casinos, A.). BIOS Scientific Publishers Ltd., Oxford, England.

Wilga, C. & Motta, P. 1998. Conservation and variation in the feeding mechanism of the spiny dogfish *Squalus acanthias*. Journal of Experimental Biology 201: 1345-1358.

Appendices

I. Tables

Table 1 The specimens of the Spiny Dogfish Sharks included in the study, their main characteristics, and the state of their spiracles.

Catalogue #	Sex	Length	Age	Right spiracle	Left spiracle
SCM001	Female	857 mm	Mature adult	Almost closed	Almost closed
SCM002	Female	913 mm	Mature adult	Almost closed	Almost closed
SCM003	Female	1023 mm	Mature adult	Closed	Closed
SCM004	Female	959 mm	Mature adult	Almost closed	Almost closed
SCM005	Female	106 mm	Mature adult	Open	Open
SCM006	Male	715 mm	Small adult	Open	Open
SCM007	Female	688 mm	Small adult	Almost closed	Half closed
SCM008	Male	651 mm	Juvenile	Almost closed	Half closed

II. Figures

Figure 1. Left lateral view of the Spiny Dogfish Shark, *Squalus acanthias* (SCM001; almost closed spiracle), to show the position of the spiracle. (A) The head, branchial region, and pectoral fin. (B) Close-up view. Abbreviations: E = eye ball, GS = second gill slit, N = naris, PF = pectoral fin, PO = pit organs, PO' = pores of the mandibular pit organs, SP = spiracle.

Figure 2. Mesoscopic images of intact left spiracles in different specimens of the Spiny Dogfish Shark, *Squalus acanthias*, to show the varying degrees of spiracular aperture and positions of the spiracular flap. (A) SCM005 with open spiracle. (B) SCM006 with open spiracle. (C) SCM008 with half closed spiracle. (D) SCM007 with half closed spiracle. (E) SCM004 with almost closed spiracle. (F) SCM002 with almost closed spiracle. (G) SCM001 with almost closed spiracle. (H) SCM003 with closed spiracle. Abbreviations: CE = caudal edge of spiracle, DE = dorsal edge of spiracle, PB = pseudobranch, RE = rostral edge of spiracle, SF = spiracular flap, SS = scaleless skin, TE = thin epithelium of spiracular canal, VE = ventral edge of spiracle.

Figure 3. Mesoscopic image of the intact and open left spiracle of the Spiny Dogfish Shark, *Squalus acanthias* (SCM006), to show the vascularized pseudobranch and the transition from the external scaly skin to the thin scaleless epithelium lining the spiracular canal. Abbreviations: CE = caudal edge of spiracle, DE = dorsal edge of spiracle, GM = scar, PB = pseudobranch, RE = rostral edge of spiracle, SF = spiracular flap, SG = spiracular groove along the caudal edge of the spiracle, TE = thin epithelium of spiracular canal, VE = ventral edge of spiracle, TF = tangential folds along the ventral edge.

Figure 4. Mesoscopic image of the intact, half-closed left spiracle in the Spiny Dogfish Shark, *Squalus acanthias* (SCM008), to show the tangentially-folded soft skin along the ventral edge of the spiracle and the spiracular groove lined with smooth epithelium along the caudal edge of the spiracle, whose shape corresponds to the counter-shape of the curved spiracular flap. Abbreviations: CE = caudal edge of spiracle, DE = dorsal edge of spiracle, PB = pseudobranch, RE = rostral edge of spiracle, SF = spiracular flap, SG = scaleless spiracular groove along the caudal edge of spiracle, TE = thin epithelium of spiracular canal, TF = tangential folds along the ventral edge of spiracle, VE = ventral edge of spiracle.

Figure 5. Mesoscopic image of the open left spiracle in the Spiny Dogfish Shark, *Squalus acanthias* (SCM006), after removal of most of the scaly skin to expose the underlying superficial fascia with its collagenous fibers. The craniodorsal superficial collagen fibers (DF) run from caudoventral to craniodorsal, and the caudodorsal superficial collagen fibers (CF) run from cranioventral to caudodorsal. Some skin (SK) adhered to the superficial fascia and could not be removed with the rest of the skin. Abbreviations: CE = caudal edge of spiracle, CF = caudodorsal fascia, DE = dorsal edge of spiracle, E = eye ball, PB = pseudobranch, PO = pores of pit organs, PO' = pores of the mandibular pit organs, RE = rostral edge of spiracle, SC = scaly skin, SF = spiracular flap, SG = scaleless spiracular groove along the caudal edge of spiracle, SK = skin, SS = scaleless skin, TE = thin epithelium of spiracular canal, TF = tangential folds along

the ventral edge of spiracle, VE = ventral edge of spiracle, VF = fat along the ventral edge of spiracle.

Figure 6. Mesoscopic images of the progressively dissected open left spiracle and surrounding structures of the Spiny Dogfish Shark, *Squalus acanthias* (SCM006). (A) The superficial fascia is removed from the rostral side of the spiracle to reveal underlying structures. The marginal cartilage, which supports the rostral and dorsal edges of the spiracle, is isolated, but left attached to the superficial fascia. The spiracular pouch is left intact. (B) The superficial fascia is completely removed, except for the attachment of the marginal cartilage in the caudodorsal corner of the spiracle. (C) The marginal cartilage is removed to reveal the entire spiracular pouch and spiracular flap, which is underlain by the spiracular muscle. The border between the spiracular muscle and levator hyomandibulae muscle is more clearly visible. Abbreviations: AM = adductor mandibulae muscle, ASA = afferent spiracular artery, C = marginal cartilage, CA = attachment sites of the marginal cartilage to the superficial fascia, CE = caudal edge of spiracle, CF = caudodorsal fascia, CLH = caudal levator hyomandibulae muscle, E = eye ball, FB = cut border of the superficial fascia, HM = hyomandibula, HT = hyomandibular nerve trunk, LP = levator palatoquadrati muscle, PO' = pores of mandibular pit organs, PAM = adductor mandibulae process, PB = pseudobranch, POM = preorbital muscle, POP = postorbital process of chondrocranium, SC = scaly skin, SF = spiracular flap, SG = spiracular groove along the caudal edge of spiracle, SM = spiracular muscle, SP = spiracular pouch, SRH = superficial portion of the rostral levator hyomandibulae muscle, TAM = surface tendon of the complexly pinnate adductor mandibulae muscle, TE = thin epithelium of the spiracular canal.

Figure 7. Mesoscopic image of the intact muscles surrounding the spiracle of the Spiny Dogfish Shark, *Squalus acanthias* (SCM006), after removal of the spiracular pouch and the epithelial lining the external part of the spiracular canal to reveal the entire spiracular muscle, which forms the spiracular flap. The thick hyomandibular nerve trunk of the facial nerve is seen emerging from the chondrocranium, and some subdivisions of the large adductor mandibulae muscle are visible. Abbreviations: AM = adductor mandibulae muscle, ASA = afferent spiracular artery, CLH = caudal levator hyomandibulae muscle, E = eye ball, HM = hyomandibula, HT = hyomandibular nerve trunk, LH = levator hyomandibulae muscle, LP = levator palatoquadrati muscle, PAM = adductor mandibulae process, PB = pseudobranch, POP = postorbital process of chondrocranium, RL = rostral spiracular ligament, SC = scaly skin, SM = spiracular muscle, SRH = superficial portion of the rostral levator hyomandibulae muscle, TAM = surface tendon of the complexly pinnate adductor mandibulae muscle, TE = thin epithelium of the spiracular canal.

Figure 8. Macroscopic images of the left branchiomeric muscles surrounding the open spiracle in the Spiny Dogfish Shark, *Squalus acanthias* (SCM006). (A) After removal of the superficial fascia. (B) Same region as in A after reflection of the adductor mandibulae muscle and tendon. Abbreviations: ALC = accessory labial cartilage, AM = adductor mandibulae muscle, AM' = reflected adductor mandibulae muscle, ASA = afferent spiracular artery, BTC = branchial trematic constrictor muscle, C = marginal cartilage, CLH = caudal levator hyomandibulae

muscle, CM = cucullaris muscle, DHC = dorsal hyoid constrictor muscle, DLC = dorsal labial cartilage, E= eye ball, GS = second gill slit, HM = hyomandibula, HT = hyomandibular trunk, HTC = hyoid trematic constrictor muscle, IM = intermandibular muscle, LP = levator palatoquadrati muscle, MB = mandibular branch of the trigeminal nerve (V), MC = mandibular cartilage, N = naris, P = palatoquadrate cartilage, PAM = adductor mandibulae process, POM = preorbital muscle, POP = postorbital process of chondrocranium, RTF = reflected tendon of the adductor mandibulae muscle, SC = scaly skin, SF = spiracular flap, SM = spiracular muscle, SP = spiracular pouch, SRH = superficial portion of the rostral levator hyomandibulae muscle, TAM = tendon of the adductor mandibulae muscle, TP = tendinous plate of the hyoid constrictor muscle, VHC = ventral hyoid constrictor muscle.

Figure 9. Mesoscopic image of the muscles on the rostro-ventral side of the open spiracle of the Spiny Dogfish Shark, *Squalus acanthias* (SCM006), after removal of the superficial fascia and reflection of the bisected superficial tendon of the adductor mandibulae muscle. Abbreviations: ALH = aponeurosis of the rostral levator hyomandibulae muscle, AM = adductor mandibulae muscle, CET = cut edge of the superficial tendon of the adductor mandibulae muscle, HT = hyomandibular nerve trunk, HM = hyomandibula, LP = levator palatoquadrati muscle, PAM = adductor mandibulae process, PB = pseudobranch, PN = pinhead, POM = preorbital muscle, POP = postorbital process of the chondrocranium, RL= rostral spiracular ligament, RTF = reflected tendon of the adductor mandibulae muscle, SC = scaly skin, SM = spiracular muscle, SRH = superficial portion of the rostral levator hyomandibulae muscle, TPM = tendon of the preorbital muscle, VL = ventral spiracular ligament.

Figure 10. Mesoscopic images of the ventral part of the open spiracle in the Spiny Dogfish Shark, *Squalus acanthias* (SCM006), after removal of the superficial fascia. (A) After removal of the epithelium from the spiracular canal to expose the hyomandibular nerve trunk emerging from the chondrocranium. (B) After removal of the hyomandibular nerve trunk to show the indentation left on the levator hyomandibulae muscle. Abbreviations: ALH = aponeurosis of the rostral levator hyomandibulae muscle, AM = adductor mandibulae muscle, CLH = caudal levator hyomandibulae muscle, HT = hyomandibular nerve trunk, HM = hyomandibula, IN = indentation left by the hyomandibular nerve trunk, LP = levator palatoquadrati muscle, MB = mandibular branch of the trigeminal nerve (V), PAM = adductor mandibulae process, PB = pseudobranch, POP = postorbital process, RL = rostral spiracular ligament, SM = spiracular muscle, SRH = superficial portion of the rostral levator hyomandibulae muscle, TE = thin epithelium of the spiracular canal.

Figure 11. Mesoscopic image of the open spiracle of the Spiny Dogfish Shark, *Squalus acanthias* (SCM006), after the removal of the thin epithelium from the spiracular wall to reveal the point of emergence of the hyomandibular nerve trunk from the chondrocranium. Abbreviations: ALH = aponeurosis of the rostral levator hyomandibulae muscle, AM = adductor mandibulae muscle, CH = chondrocranium, CLH = caudal levator hyomandibulae muscle, HT = hyomandibular nerve trunk, HM = hyomandibula, LP = levator palatoquadrati muscle, LW = cut

border of the epithelial lining of the spiracular wall, MB = mandibular branch of the trigeminal nerve (V), PAM = adductor mandibulae process, PB = pseudobranch, PI = point of emergence of the hyomandibular nerve trunk, POP = postorbital process of the chondrocranium, SM = spiracular muscle, SRH = superficial portion of the rostral levator hyomandibulae muscle, RL = rostral spiracular ligament.

Figure 12. Mesoscopic image of the insertions of the preorbital muscle onto the adductor mandibulae muscle in the Spiny Dogfish Shark, *Squalus acanthias* (SCM006). Notice the mandibular branch of the trigeminal nerve (V) traveling along the rostral side of the adductor mandibulae muscle and then separating the lateral and medial tendons of the preorbital muscle. Abbreviations: AM = adductor mandibulae muscle, DLC = dorsal labial cartilage, LT = lateral tendon of the preorbital muscle, MB = mandibular branch of the trigeminal nerve (V), MT = medial tendon of the preorbital muscle, POM = preorbital muscle.

Figure 13. Mesoscopic image of the insertions of the preorbital muscle onto the medial side adductor mandibulae muscle and the surface of the mandibular arch in the Spiny Dogfish Shark, *Squalus acanthias* (SCM006), once the adductor mandibulae muscle was reflected. Notice the small deep tendon of the preorbital muscle (DT) inserting onto the surface of the mandibular arch. The full length of the mandibular branch of the trigeminal nerve (V) and the insertion of the medial tendon onto the medial surface of the adductor mandibulae muscle are now visible. Abbreviations: AM' = reflected adductor mandibulae muscle, DLC = dorsal labial cartilage, DT = deep tendon of the preorbital muscle, E = eye ball, MB = mandibular branch of the trigeminal nerve (V), MT = medial tendon of the preorbital muscle, P = palatoquadrate, POM = preorbital muscle, RTF = reflected tendon of the adductor mandibulae muscle and superficial fascia, SC = scaly skin.

Figure 14. Mesoscopic rostro-lateral view of the dissected, open spiracle in the Spiny Dogfish Shark, *Squalus acanthias* (SCM006). Notice both the rostral spiracular ligament as well as the ventral spiracular ligament and their insertions onto the spiracular muscle. The adductor mandibulae has been reflected, revealing the entire palatoquadrate and its position within the branchiomeric musculature. Abbreviations: ALH = aponeurosis of the rostral levator hyomandibulae muscle, APM = articulation of the palatoquadrate and mandibular arch, ASA = afferent spiracular artery, CLH = caudal levator hyomandibulae muscle, HM = hyomandibula, LP = levator palatoquadrati muscle, P = palatoquadrate, PAM = adductor mandibulae process, POP = postorbital process of chondrocranium, RL = rostral spiracular ligament, RTF = reflected tendon of the adductor mandibulae muscle and superficial fascia, SC = scaly skin, SM = spiracular muscle, SRH = superficial portion of the rostral levator hyomandibulae muscle, VL = ventral spiracular ligament.

Figure 15. Mesoscopic caudoventral view of the open spiracle of the Spiny Dogfish Shark, *Squalus acanthias* (SCM006), after removal of the superficial fascia, to show the tendon of the superficial portion of the rostral levator hyomandibulae inserting onto the medial side of the

adductor mandibulae process of the palatoquadrate. Abbreviations: ALH = aponeurosis of the rostral levator hyomandibulae muscle, ASA = afferent spiracular artery, CH = chondrocranium, CLH = caudal levator hyomandibulae muscle, DHC = dorsal hyoid constrictor muscle, HM = hyomandibula, LP = levator palatoquadrati muscle, P = palatoquadrate, PAM = adductor mandibulae process, PB = pseudobranch, PI= point of insertion of the hyomandibular nerve trunk, POP = postorbital process of chondrocranium, TSP = tendon of the superficial portion of the rostral levator hyomandibulae muscle, SC = scaly skin, SM = spiracular muscle, SRH = superficial portion of the rostral levator hyomandibulae muscle, TAM = reflected tendon of the adductor mandibulae muscle.

Figure 16. Mesoscopic images of the open spiracle of the Spiny Dogfish Shark, *Squalus acanthias* (SCM006), to show the complex levator hyomandibulae muscle. (A) After removal of the superficial portion of the rostral levator hyomandibulae muscle to reveal the palatoquadrate part of the deep portion of the rostral levator hyomandibulae muscle. (B) After reflection of the caudal levator hyomandibulae muscle to reveal the deep portion of the rostral levator hyomandibulae muscle. Abbreviations: ALH = aponeurosis of the rostral levator hyomandibulae muscle, ASA = afferent spiracular artery, CLH = caudal levator hyomandibulae muscle, DHC = dorsal hyoid constrictor muscle, DLH = palatoquadrate part of the deep portion of the rostral levator hyomandibulae muscle, HM = hyomandibula, LP = levator palatoquadrati muscle, MB = mandibular branch of the trigeminal nerve (V), P = palatoquadrate, PB = pseudobranch, POP = postorbital process of chondrocranium, RL = rostral spiracular ligament, RTF = reflected tendon of the adductor mandibulae muscle, SC = scaly skin, SM = spiracular muscle, TE = thin epithelium of the spiracular canal, VL = ventral spiracular ligament.

Figure 17. Mesoscopic image of the open spiracle of the Spiny Dogfish Shark, *Squalus acanthias* (SCM006), after removal of part of the adductor mandibulae process and the deep portion of the rostral hyomandibulae muscle to reveal showing the entire spiracular muscle and its insertion onto the medial surface of the palatoquadrate, ventromedial to the insertion of the rostral levator hyomandibulae muscle. Abbreviations: ASA = afferent spiracular artery, DHC = dorsal hyoid constrictor muscle, HM = hyomandibula, ICH = insertion area of the caudal levator hyomandibulae muscle on the hyomandibula, ISM = insertion area of the spiracular muscle on the adductor mandibulae process, LP = levator palatoquadrati muscle, MB = mandibular branch of the trigeminal nerve (V), OCLH = reflected caudal levator hyomandibulae muscle, OSH = origin of the superficial portion of the rostral levator hyomandibulae muscle, P = palatoquadrate, PB = pseudobranch, PI= point of insertion of the hyomandibular nerve trunk, POP = postorbital process of chondrocranium, RL = rostral spiracular ligament, RTF = reflected tendon of the adductor mandibulae muscle, SC = scaly skin, SM = spiracular muscle, TE = thin epithelium of the spiracular canal.

Figure 18. Mesoscopic caudodorsal view of the open spiracle of the Spiny Dogfish Shark, *Squalus acanthias* (SCM006), with view of the internal surface of the spiracular flap and the insertion of the spiracles muscle on the medial side of the adductor mandibulae process, as well

as the afferent spiracular artery supplying the pseudobranch, which is drained by the efferent spiracular artery. Abbreviations: ASA = afferent spiracular artery, ESA = efferent spiracular artery, HM = hyomandibula, ISM = insertion of the spiracular muscle, LP= levator palatoquadrati muscle, MB = mandibular branch of the trigeminal nerve (V), OSH = origin of the superficial portion of the rostral levator hyomandibulae muscle, P = palatoquadrate, PB = pseudobranch, POP = postorbital process of chondrocranium, RTF = reflected tendon of the adductor mandibulae muscle, SC = scaly skin, SM = spiracular muscle, SMC = spiracular cartilages, TE = thin epithelium of the spiracular canal.

Figure 19. Mesoscopic dorsal view of the open spiracle in the Spiny Dogfish Shark, *Squalus acanthias* (SCM006), after removal of the pseudobranch and efferent spiracular artery to reveal the entire length of the two spiracular cartilages, which stabilize the spiracular flap on its internal side. Abbreviations: ASA = afferent spiracular artery, DHC = dorsal hyoid constrictor muscle, HM = hyomandibula, ICH = insertion area of the caudal levator hyomandibulae muscle on the hyomandibula, ISM = insertion of the spiracular muscle, LP = levator palatoquadrati muscle, OSH = origin of the superficial portion of the rostral levator hyomandibulae muscle, P = palatoquadrate, POP = postorbital process of chondrocranium, RTF = reflected tendon of the adductor mandibulae muscle, SC = scaly skin, SM = spiracular muscle, SMC = cartilages of the spiracular muscle, TE = thin epithelium of the spiracular canal, VL = ventral spiracular ligament.

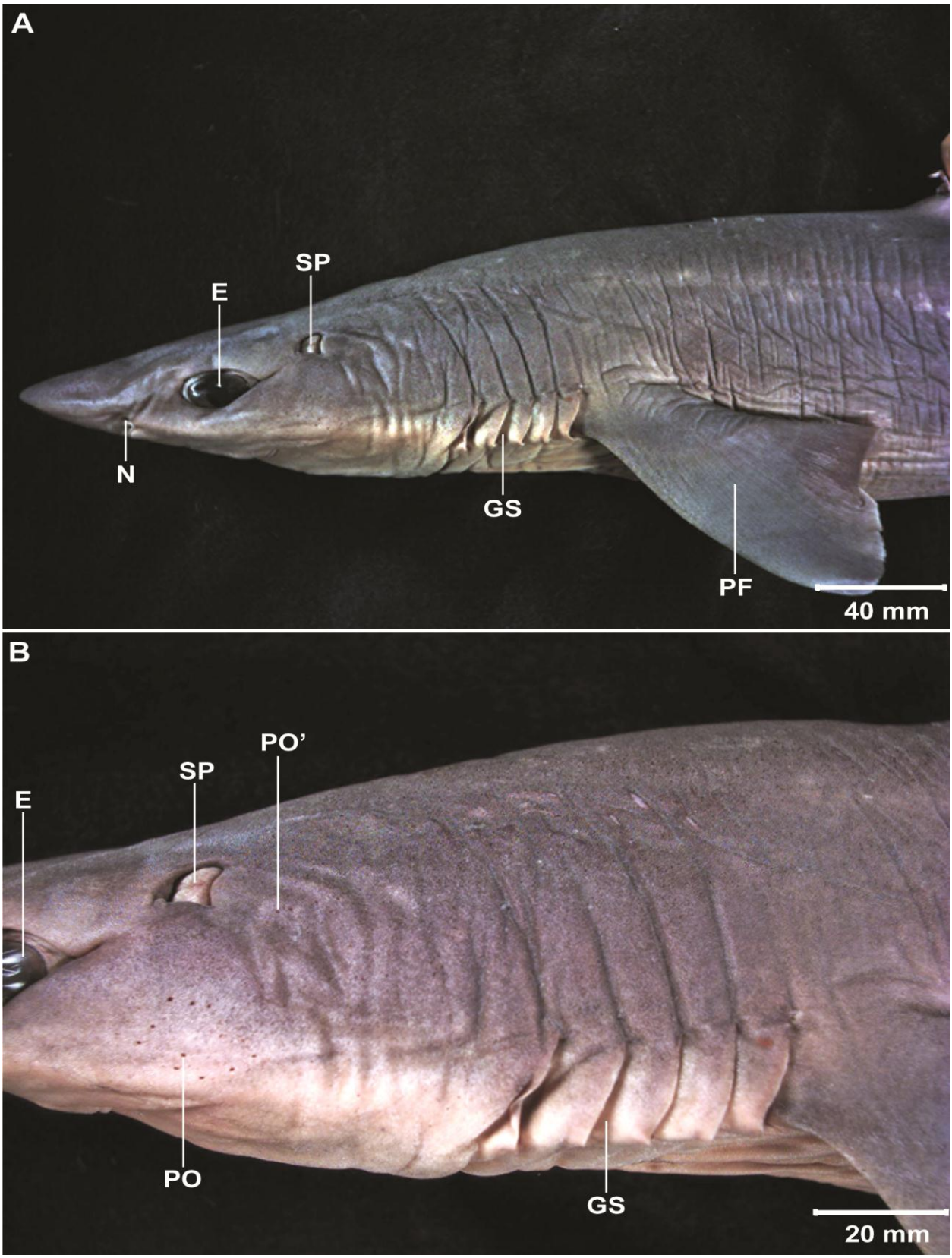

Fig. 1

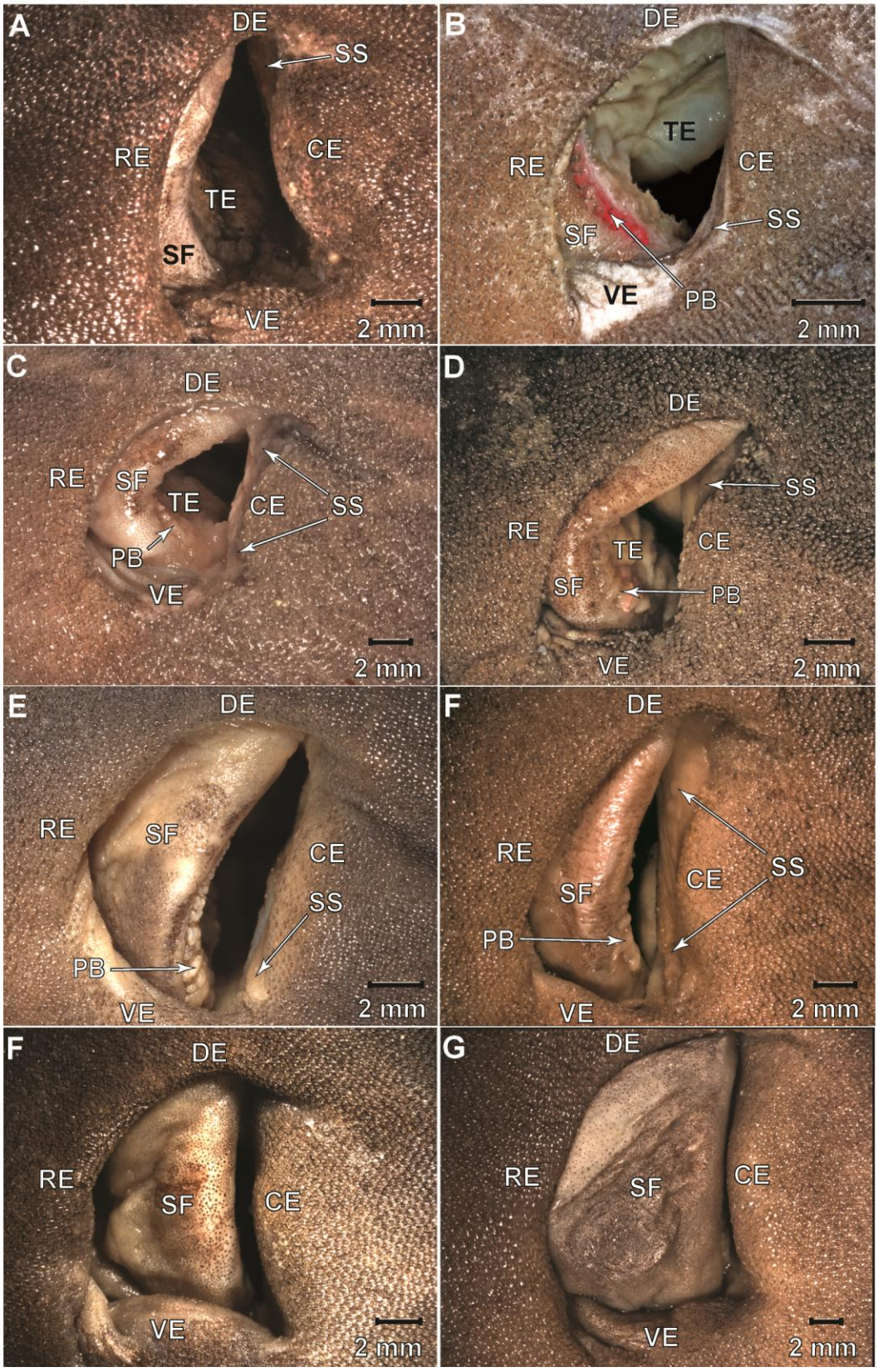
A
DE
SS
RE
CE
TE
SF
VE
2 mm
B
DE
TE
RE
CE
SS
SF
VE
PB
2 mm
C
DE
RE
SF
TE
CE
SS
PB
VE
2 mm
D
DE
SS
RE
TE
CE
SF
PB
VE
2 mm
E
DE
RE
SF
CE
SS
PB
VE
2 mm
F
DE
RE
SF
CE
SS
PB
VE
2 mm
F
DE
RE
SF
CE
VE
2 mm
G
DE
RE
SF
CE
VE
2 mm

Fig. 2

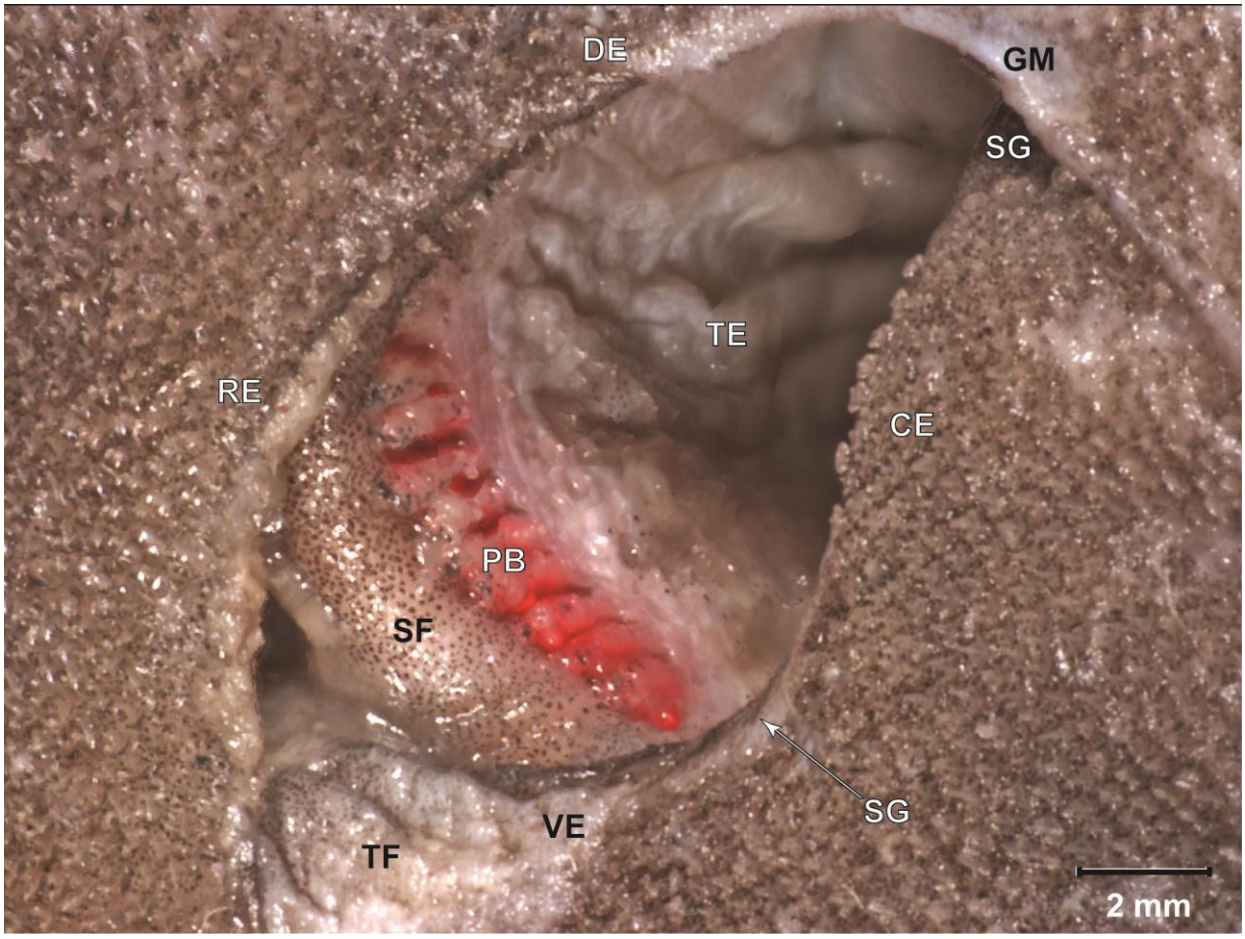

Fig. 3

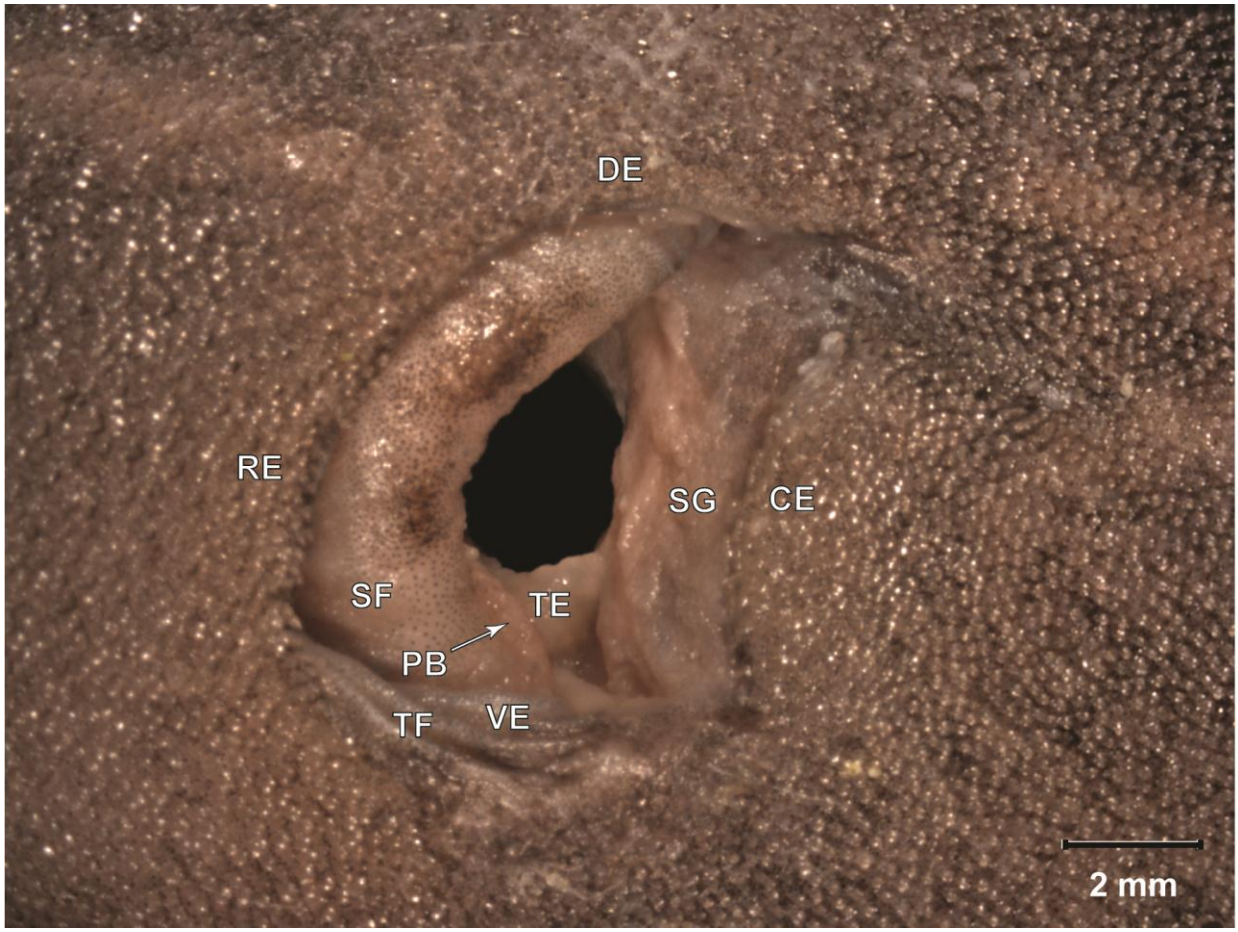

Fig. 4

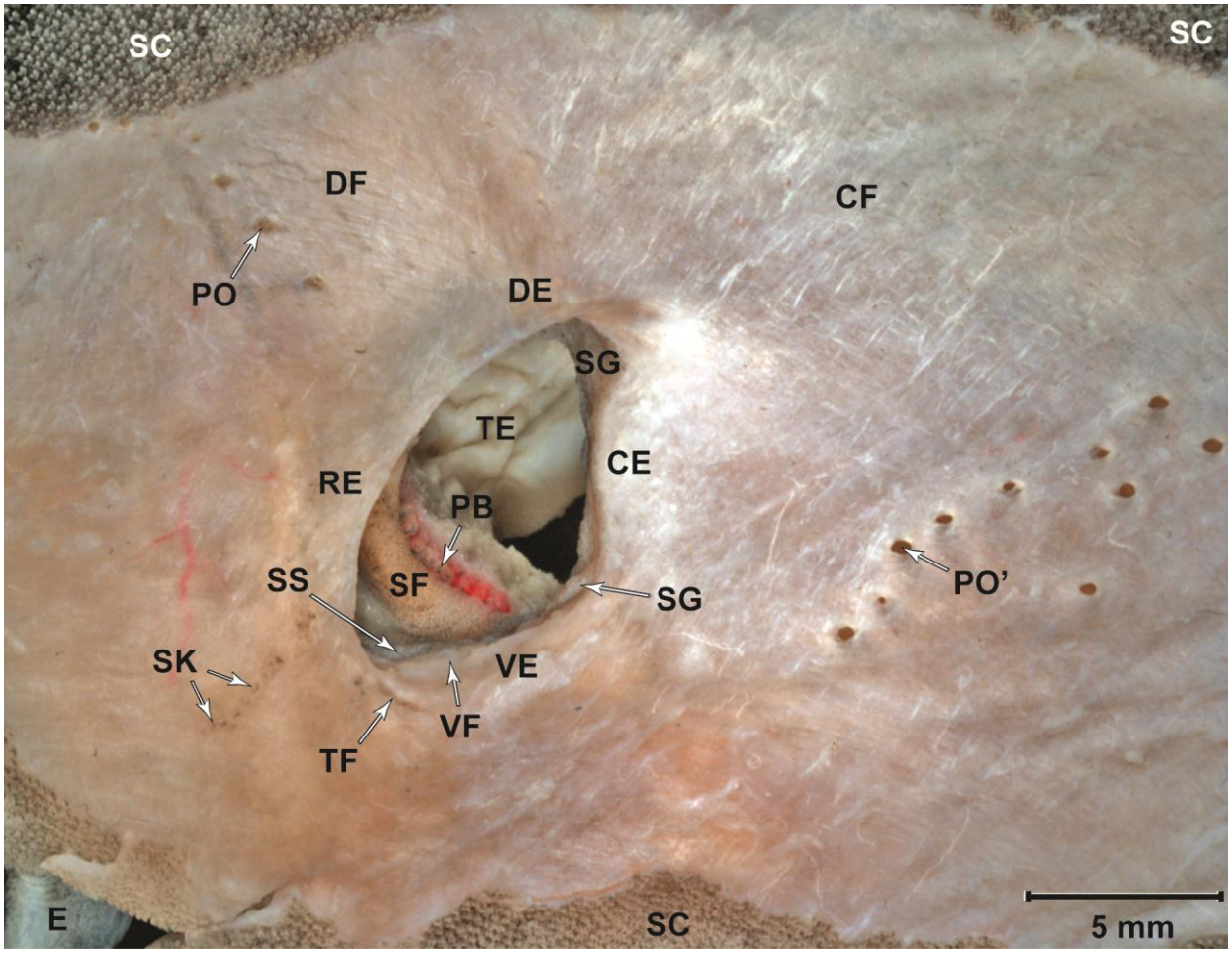

Fig. 5

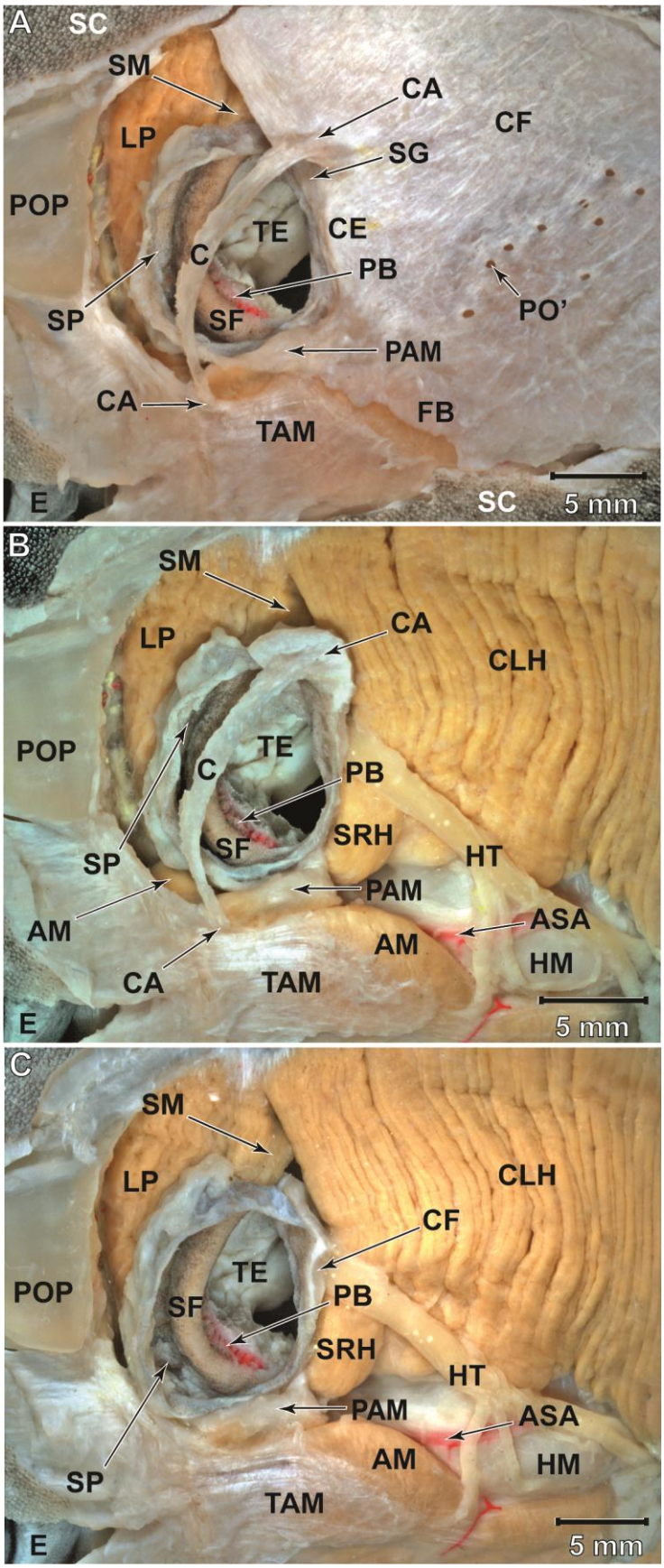
A
SC
SM
CA
CF
LP
SG
POP
TE
CE
C
PB
SP
SF
PO'
PAM
CA
FB
TAM
E
SC
5 mm
B
SM
CA
LP
CLH
POP
TE
C
PB
SRH
SF
HT
SP
PAM
AM
ASA
AM
HM
CA
TAM
E
5 mm
C
SM
CLH
LP
CF
TE
POP
SF
PB
SRH
HT
PAM
ASA
AM
HM
SP
TAM
E
5 mm

Fig. 6

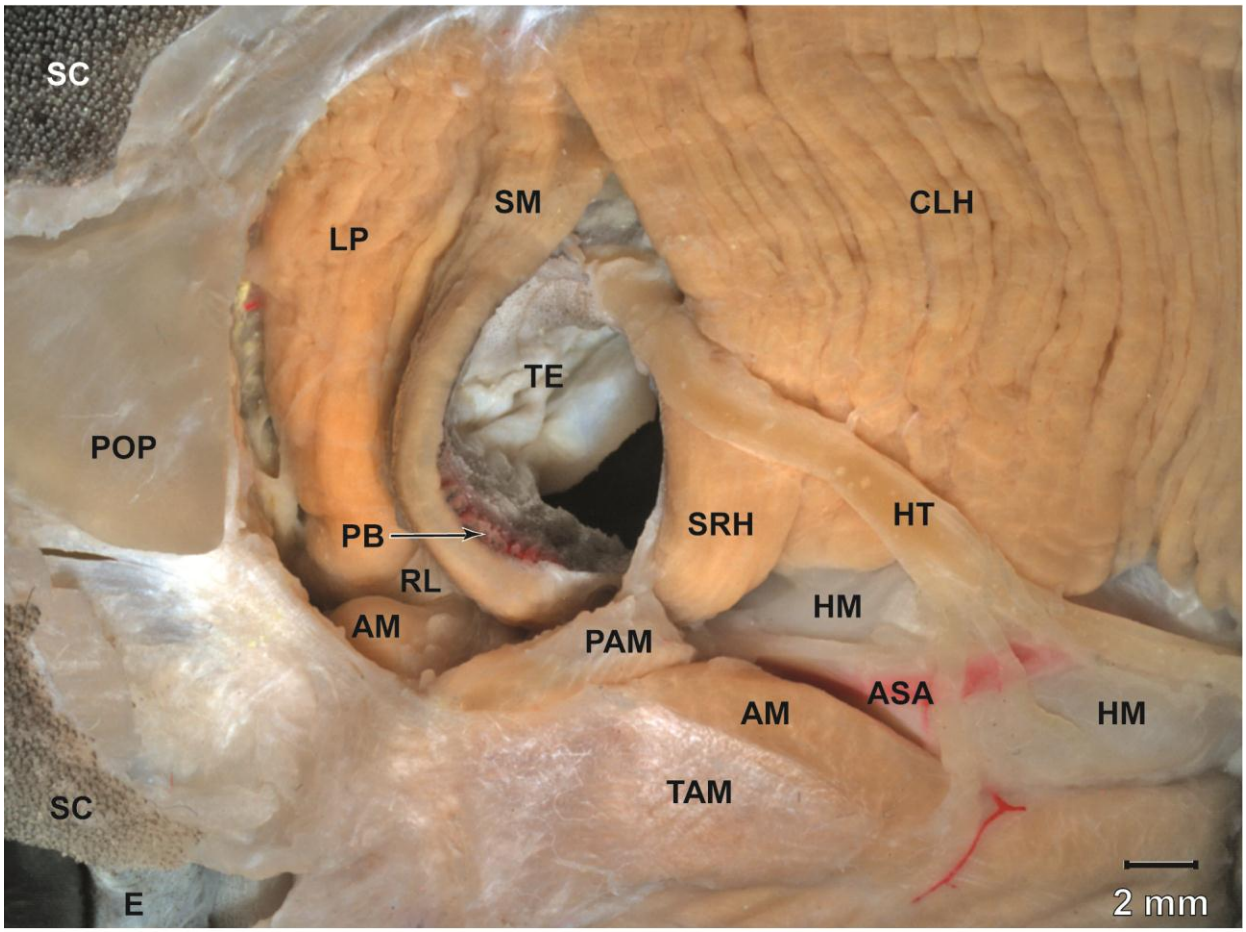

Fig. 7

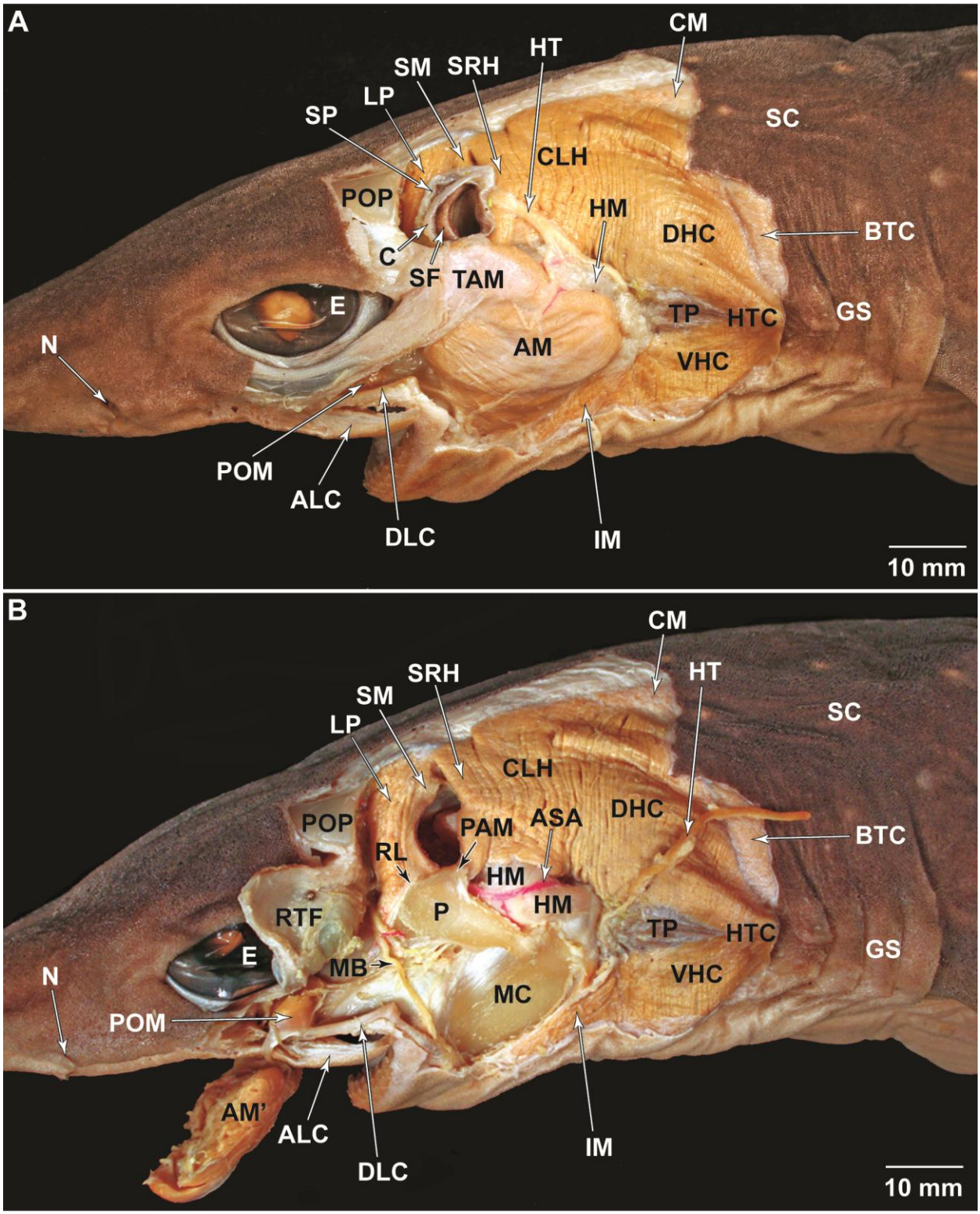
A
CM
HT
SM
SRH
LP
SP
SC
CLH
POP
HM
DHC
BTC
C
SF
TAM
E
TP
HTC
GS
N
AM
VHC
POM
ALC
DLC
IM
10 mm
B
CM
SRH
HT
SM
LP
SC
CLH
DHC
POP
PAM
ASA
BTC
RL
HM
RTF
P
HM
TP
HTC
GS
E
MB
VHC
N
MC
POM
AM'
ALC
IM
DLC
10 mm

Fig. 8

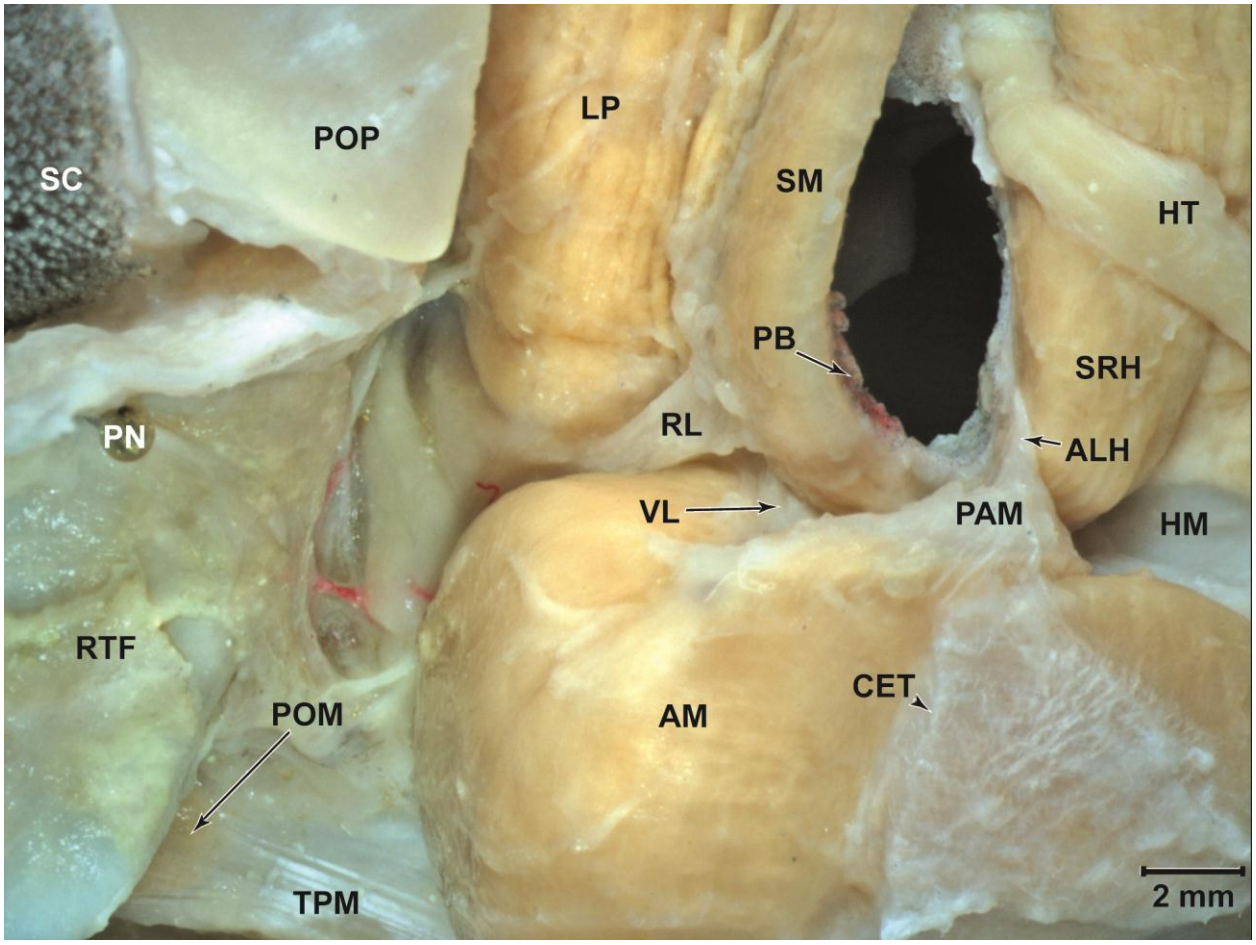

Fig. 9

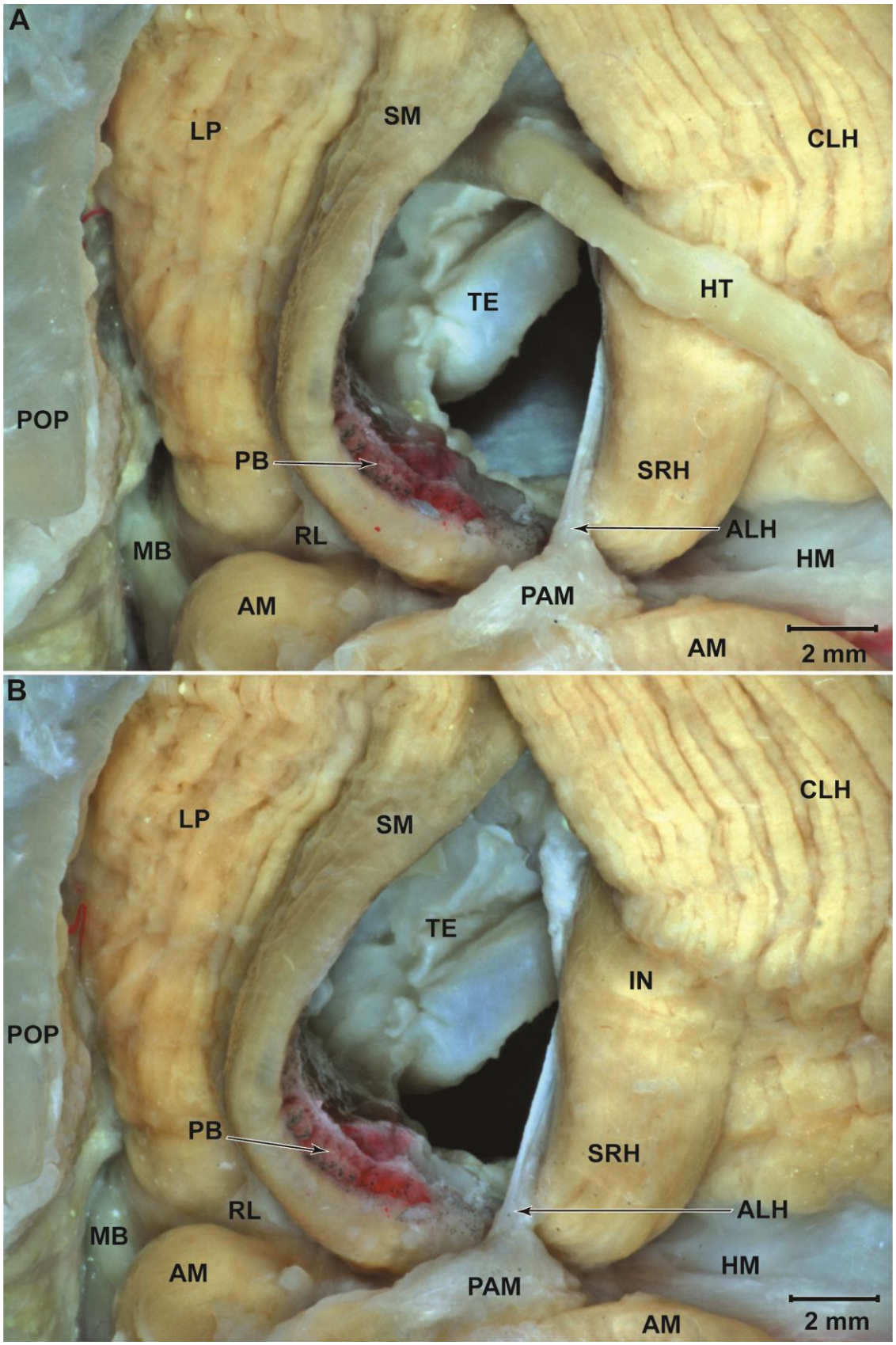
A
LP
SM
CLH
TE
HT
POP
PB
SRH
ALH
RL
MB
HM
AM
PAM
AM
2 mm
B
LP
SM
CLH
TE
IN
POP
PB
SRH
RL
ALH
MB
AM
HM
PAM
AM
2 mm

Fig. 10

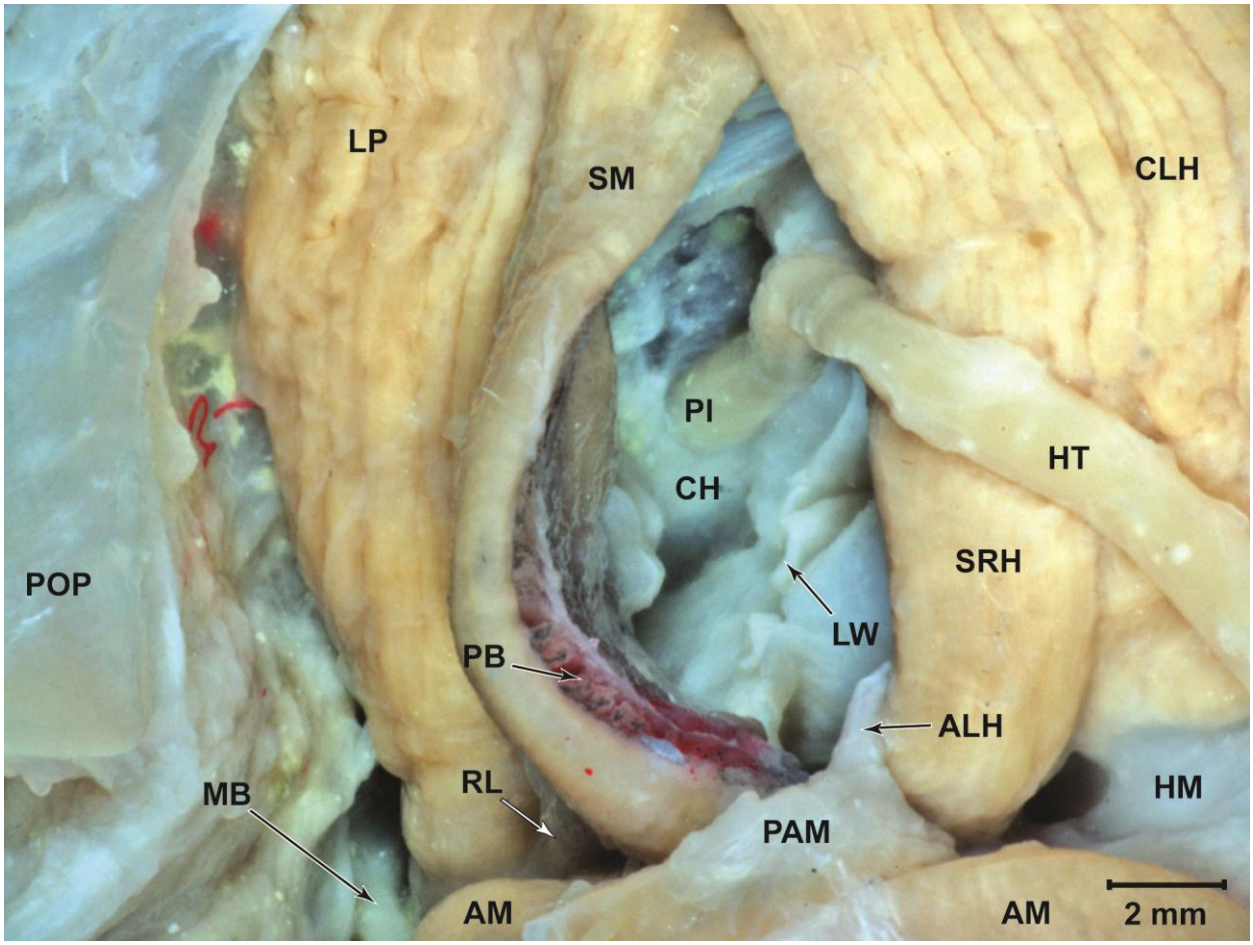

Fig. 11

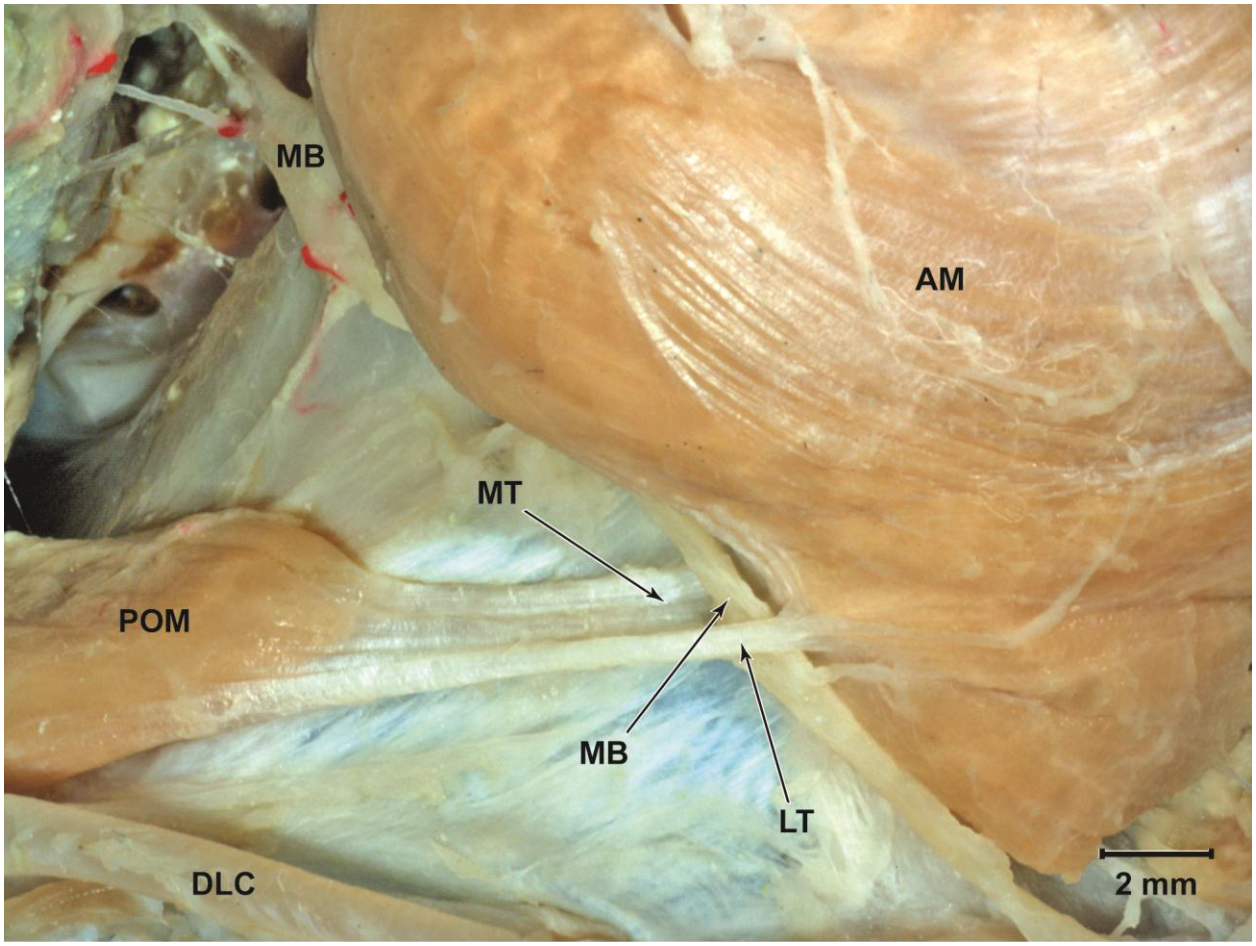

Fig. 12

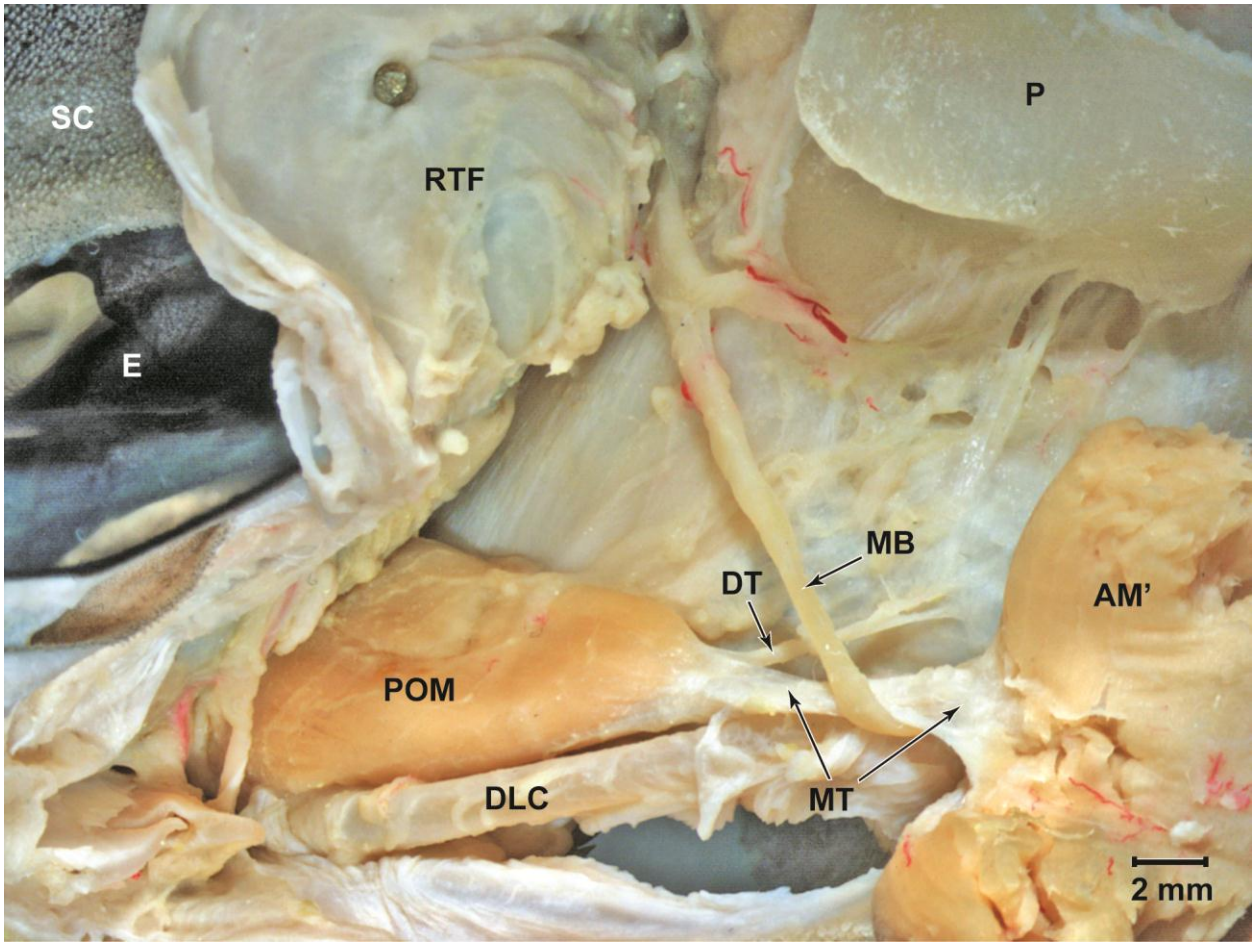

Fig. 13

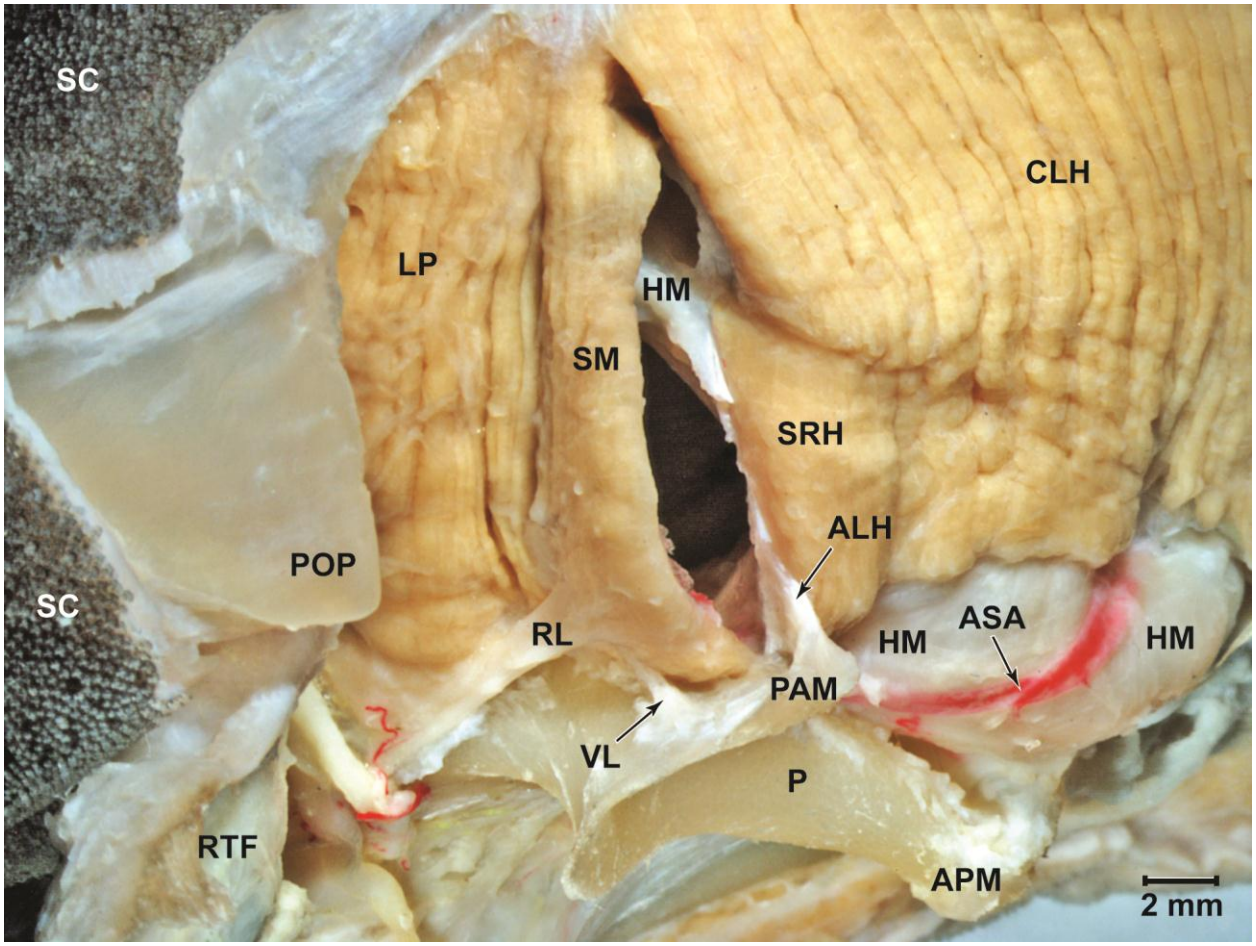

Fig. 14

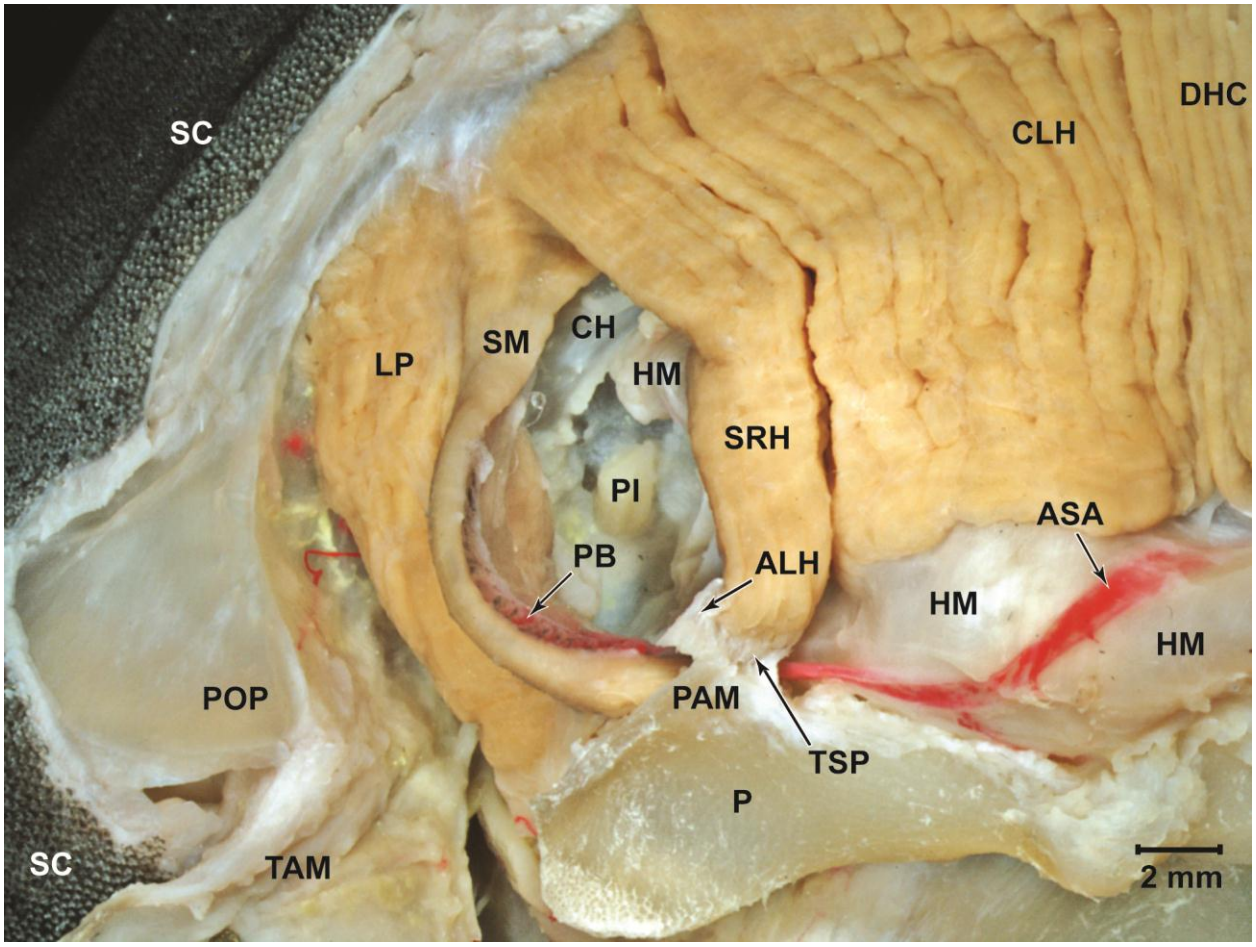
SC
DHC
CLH
LP
SM
CH
HM
SRH
PI
ASA
PB
ALH
HM
HM
POP
PAM
TSP
P
SC
TAM
2 mm

Fig. 15

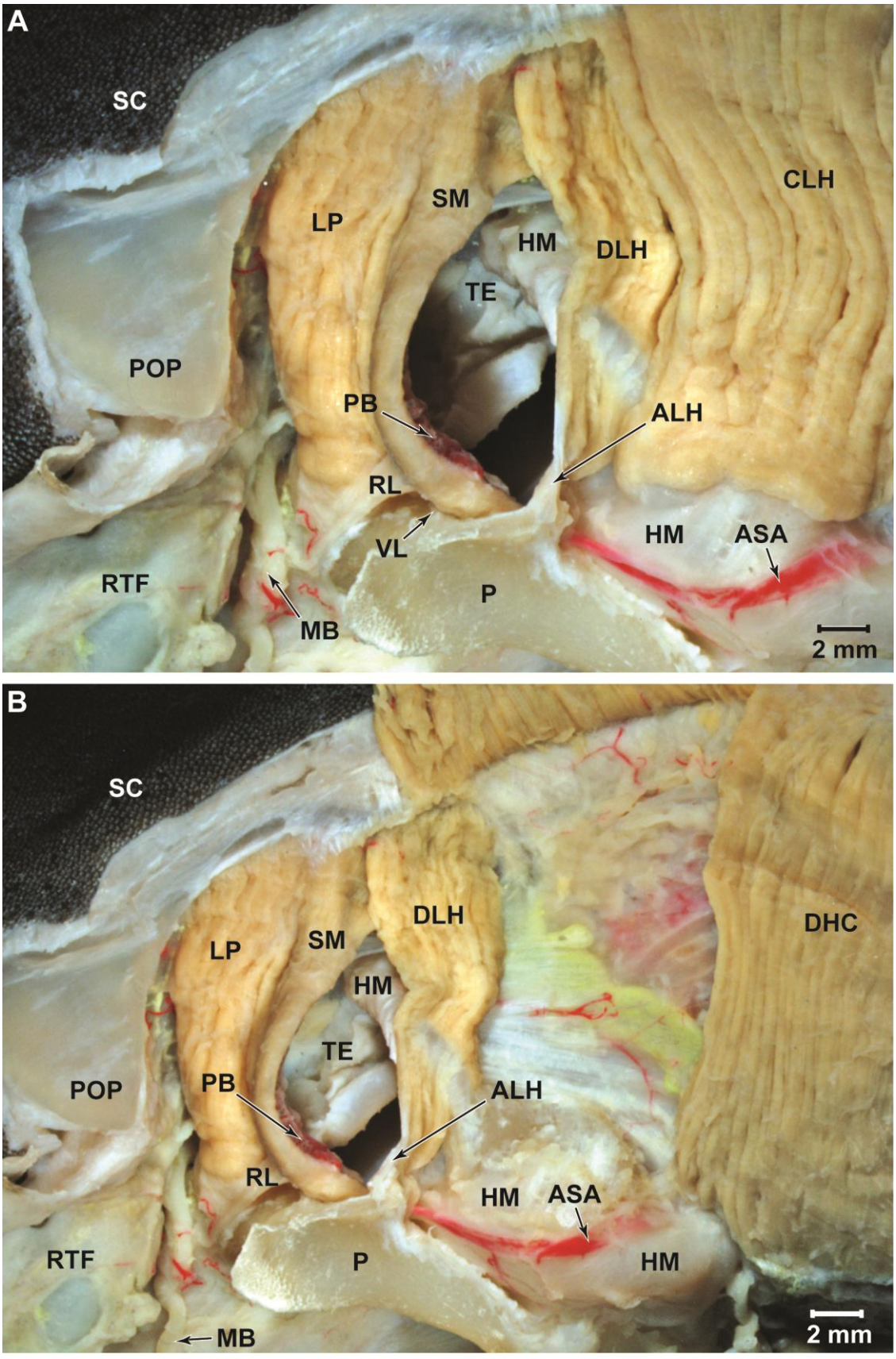
A
SC
LP
SM
HM
DLH
CLH
TE
POP
PB
ALH
RL
VL
HM
ASA
RTF
P
MB
2 mm
B
SC
DLH
DHC
LP
SM
HM
TE
POP
PB
ALH
RL
HM
ASA
RTF
P
HM
MB
2 mm

Fig. 16

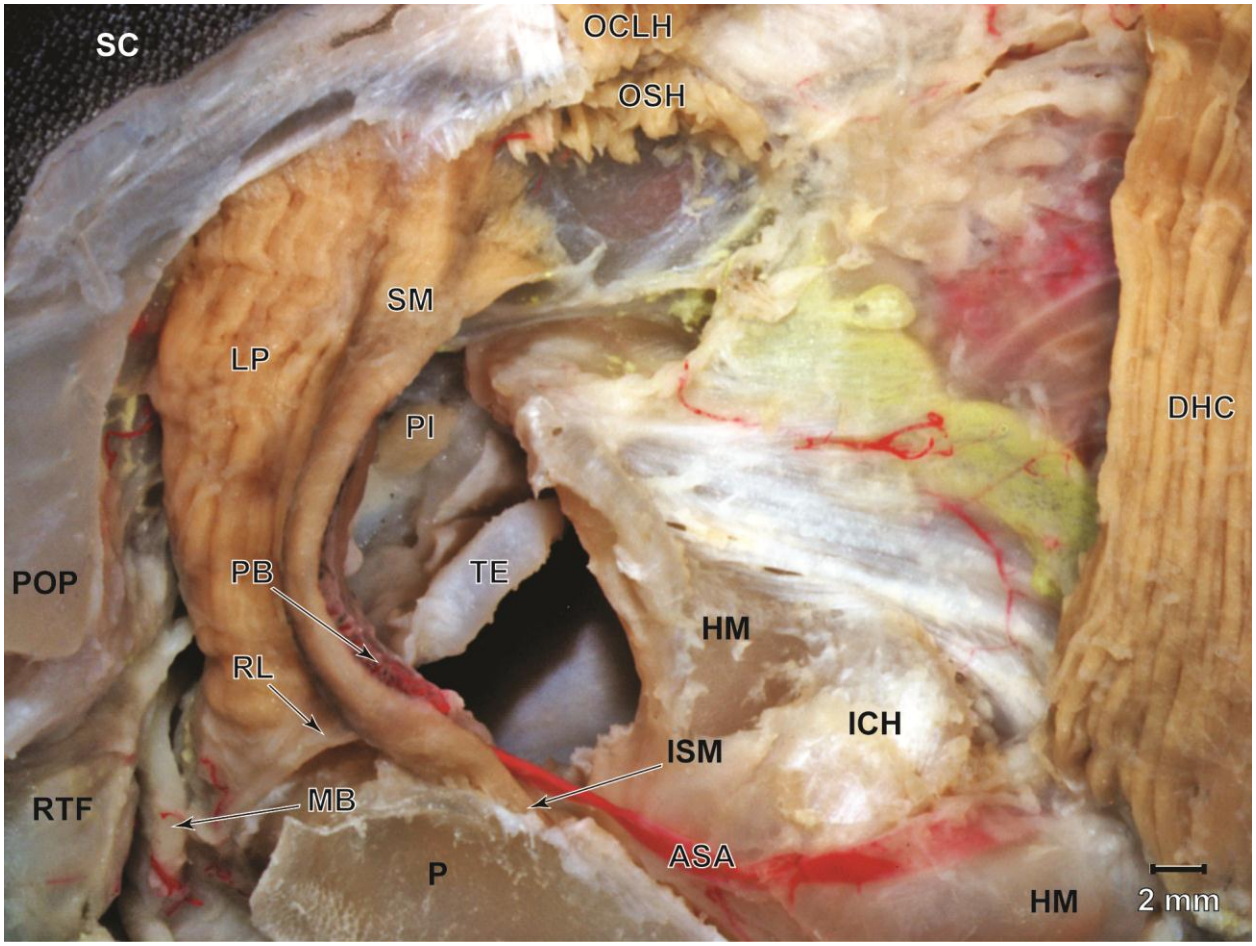

Fig. 17

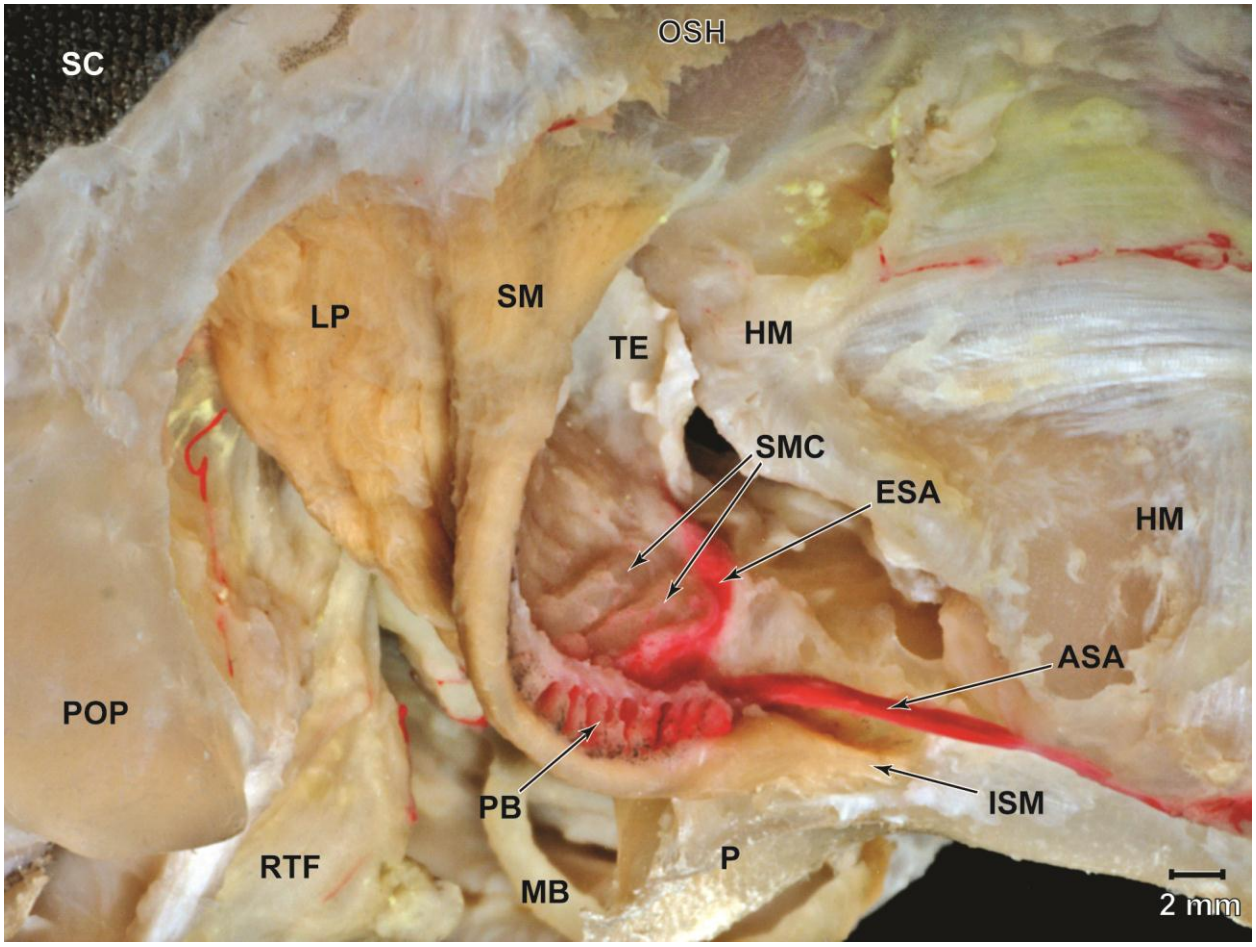

Fig. 18

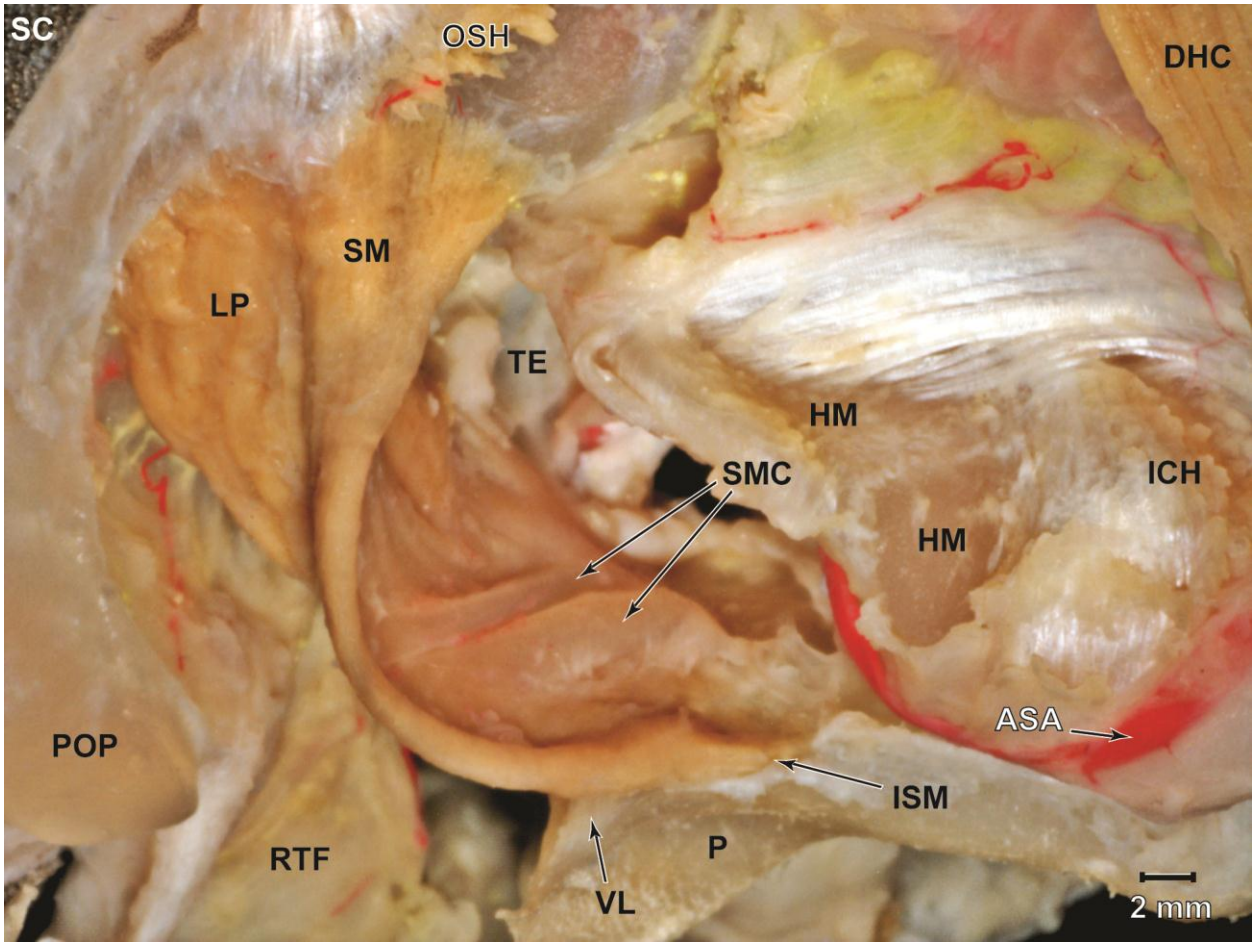

Fig. 19